

Single quantum dots as artificial atoms, quantum optics and quantum cryptography at the Tyndall National Institute.

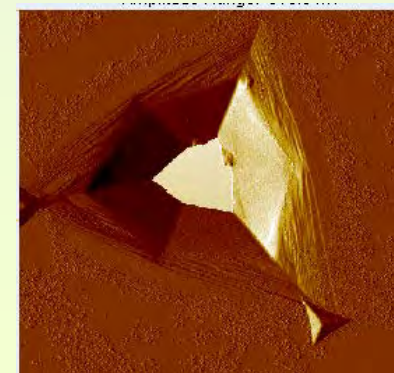
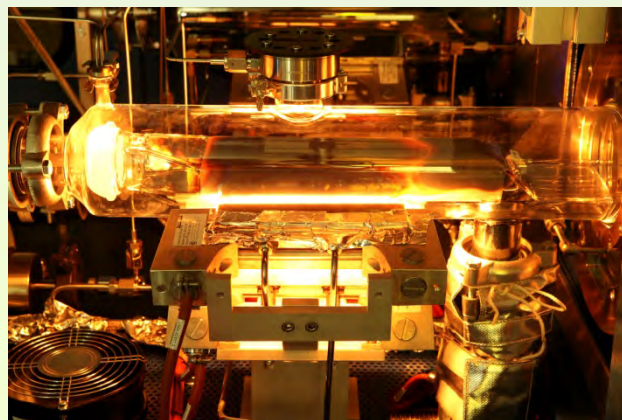
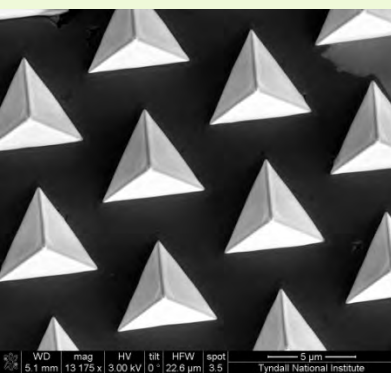


E. Pelucchi

Collaborators: T. H. Chung, G. Juska, V. Dimastrodonato, S. T. Moroni, A. Pescaglino, E. Mura and A. Gocalinska

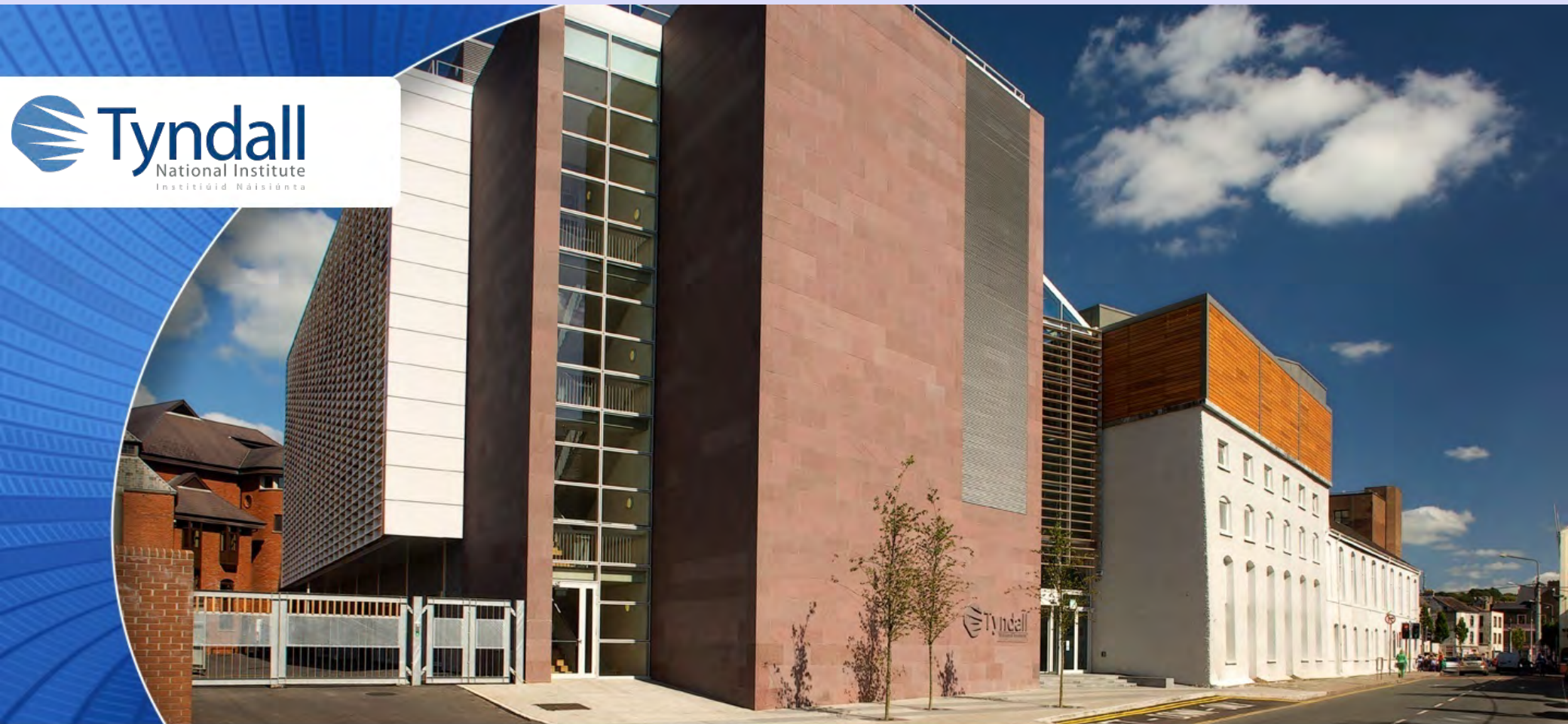


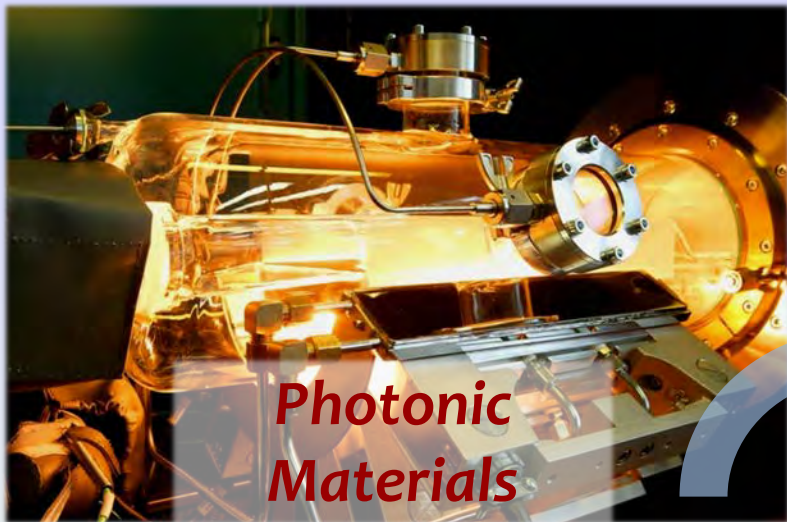
*Epitaxy and Physics of Nanostructures,
Tyndall National Institute, University College Cork,
"Lee Maltings", Dyke Parade, Cork, Ireland*



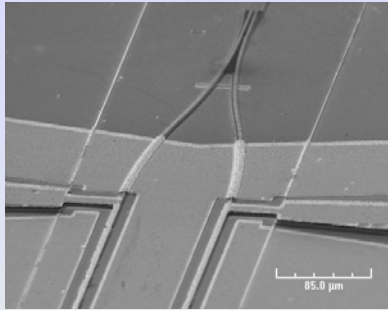
Tyndall (at University College Cork)

Excellence in ICT research

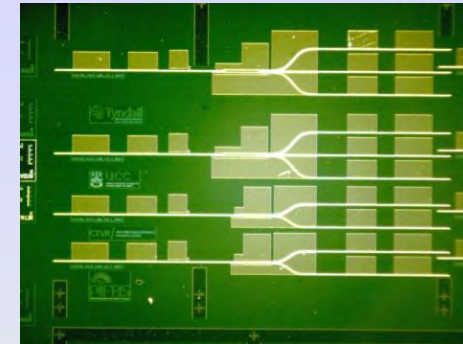
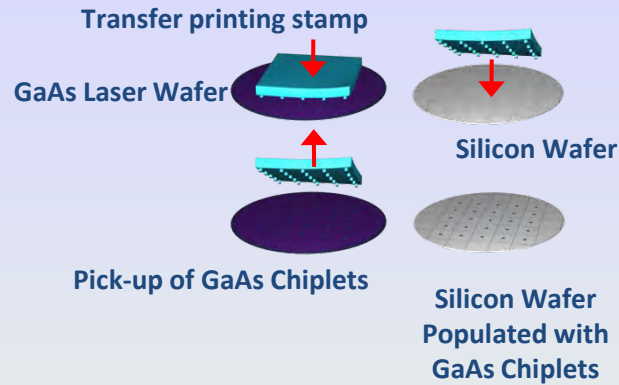




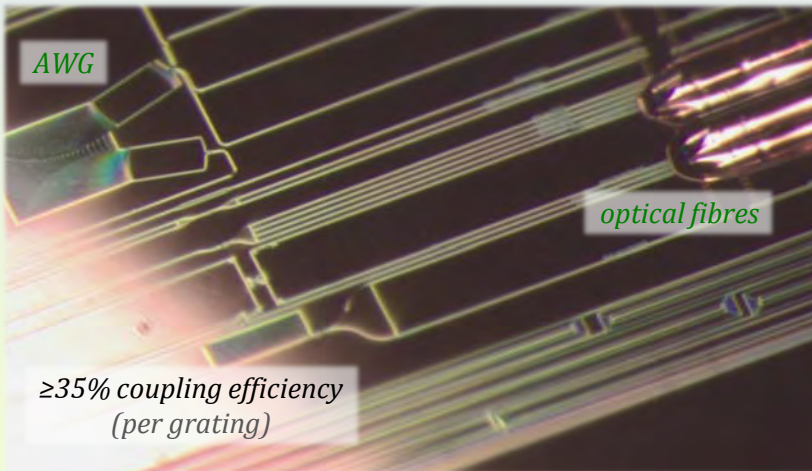
Mach-Zehnder Modulators



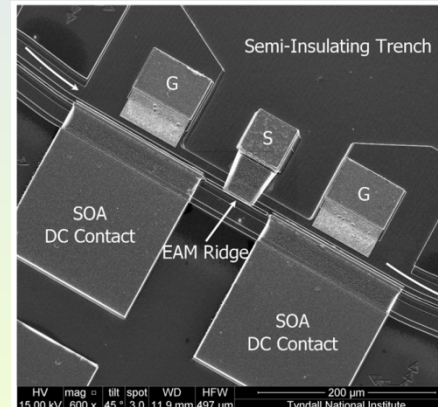
Epitaxial material transfer



Integrated DQPSK Transmitter



Fibre coupling of Silicon photonic waveguides at Tyndall
(patent application PCT/EP2011/068240)



High speed EAM integrated with SOAs

For the moment Tyndall is the only place in Ireland with experimental quantum information

W

SINGLE PHOTON INTERFERENCE IN 10km LONG OPTICAL FIBRE INTERFEROMETER

P. D. Townsend, J. G. Rarity and P. R. Tapster

Indexing terms: Interferometers, Optical communication, Cryptography

Single-photon interference fringes with greater than 90% visibility were measured using a 10km long optical fibre interferometer. The experiment employed a pulsed semiconductor laser source operating at a wavelength of 1.3 μm and a novel single-photon counting scheme using high-speed germanium avalanche photodiodes. Interferometers of this type could form the basis of future quantum cryptography systems.

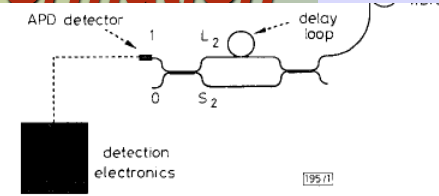


Fig. 1 Schematic diagram of single-photon time-division Mach-Zehnder interferometer

The source used in the experiment was a gain-switched semiconductor laser operating at a wavelength of 1.3 μm , which produced pulses of 30 ps duration at a repetition rate of 105 MHz. The output from this laser was strongly attenuated so that at the input to the transmission fibre the average number of photons per pulse μ was of the order of 0.1. This choice of a small μ value was required to obtain a reasonable approximation to a single photon source. In this case a laser exhibiting Poissonian photon number fluctuations produces only a small fraction of pulses $\sim \mu^2/2$ containing on average two or more photons. However, this situation is obtained at the expense of a large fraction of pulses $\sim (1 - \mu)$ containing on average zero photons [1]. After attenuation, the incoming pulses were split by the first fibre-coupler (nominally 50/50) between a short fibre path S_1 , and a longer fibre path L_1 , in order to form a temporally separated pulse pair. Path L_1 contained a phase shifter consisting of a short free space link the length of which could be varied by means of a piezoelectric transducer (PZT). The path lengths L_1 and S_1 were chosen such that a relative time delay of 1.1 ns was obtained between the pair of pulses coupled into the transmission fibre via the second coupler. After propagation through 10 km of standard communications fibre, the pulses were again split between short and long paths of length $S_2 (=S_1)$ and $L_2 (=L_1)$, respectively, and then combined at the final coupler. The output from the final coupler thus consisted of three temporal pulses each separated by 1.1 ns. The central pulse was made up of two temporally coincident components that arrived via the S_1L_2 and the L_1S_2 paths, respectively, and hence exhibited interference behaviour as the relative optical phase was varied by means of the PZT.

Single photon counting was carried out using a high-speed germanium avalanche photodiode cooled to 77 K and operating in the Geiger mode with passive quenching via a 33 k Ω resistor [8]. After amplification and leading edge-discrimination, the signals from the detector were used as start pulses for a time-interval analyser (HP 53310A). For each

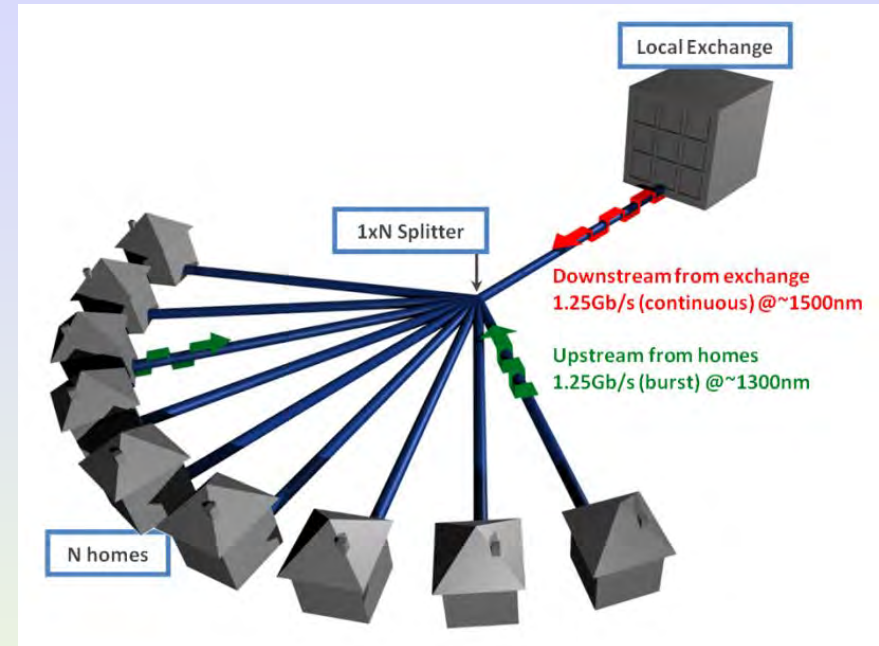
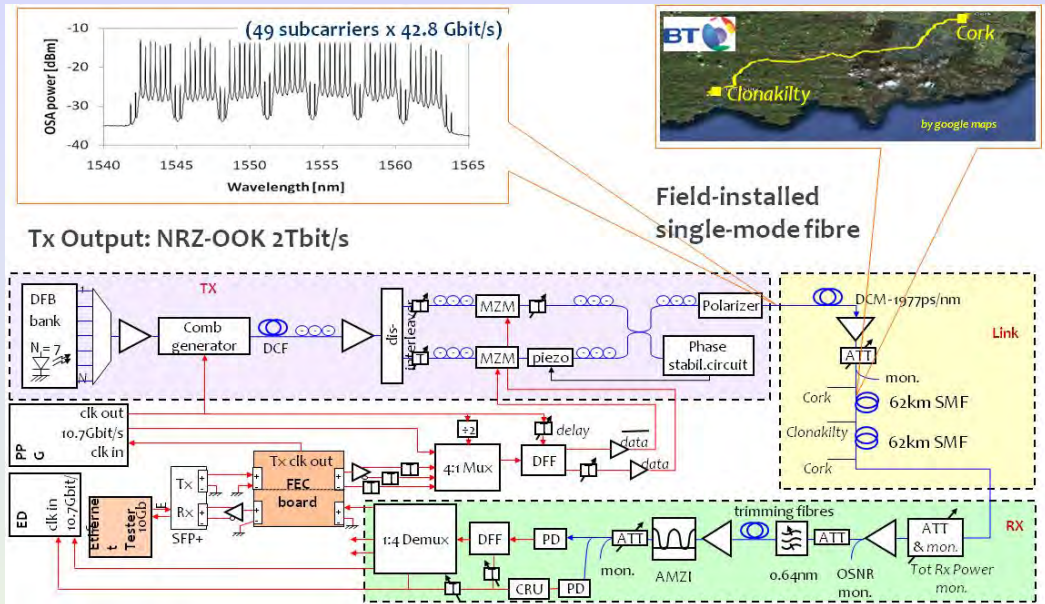


P. Townsend has pioneered quantum cryptography

The security of any key-based cryptography system depends ultimately on the secrecy of the key. Quantum cryptography is a radical new technique for the distribution of cryptographic keys which exploits the uncertainty principle of quantum mechanics to guarantee the secrecy of the key [1-5]. The implementation of this technique in the optical domain involves the transmission of a random bit sequence from a source A to a receiver B using a single photon to carry each bit of data. This binary data can be encoded using, for example, either the polarisation states [1-4] or phase states of the photons [6, 7]. Random switching between orthogonal phase or polarisation coding bases provides protection against eavesdroppers. In performing measurements on the channel, an eavesdropper causes unavoidable changes in the photon states which show up as errors when A and B perform a comparison of a fraction of the sent and received bits. If the legitimate users of the channel fail to detect an eavesdropper they can use the remaining data to generate a cryptographic key. Unlike in conventional key distribution techniques, the secrecy of the key is now guaranteed by the fundamental laws of physics.

In a recent pioneering experiment, Bennett *et al.* [1] have demonstrated the operation of a quantum cryptographic channel, which was used to transmit a secret key over a free-space link about 30 cm in length at a data rate of approximately 10 bit/s. In this Letter, we characterise the performance of an optical-fibre-based single-photon communication channel which possesses some of the important features that the transmission medium for a future quantum cryptographic system would require. As illustrated in Fig. 1, the channel takes the form of an extended time-division Mach-Zehnder interferometer [6]. In this format, the Mach-Zehnder can be very long and yet remain stable against

Photonic Systems: Extensive facilities (“best in europe”)

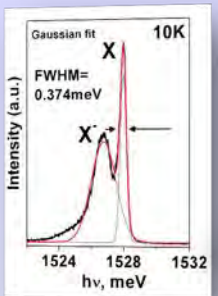
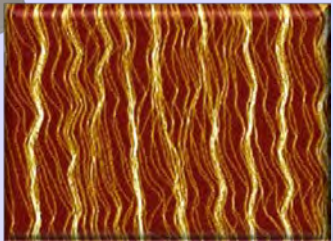


Photonic Systems: Quantum information to the home

Iris Choi, Robert J Young and Paul D Townsend, New Journal of Physics 13 (2011) 063039

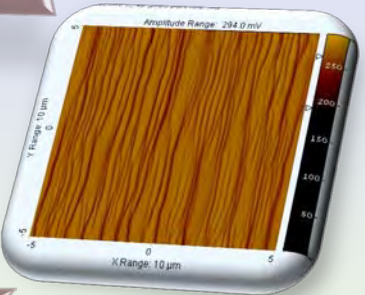
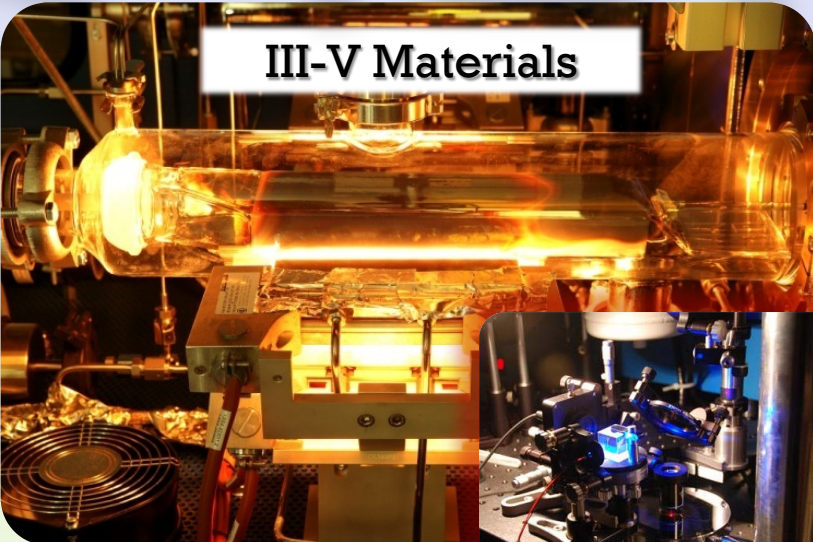
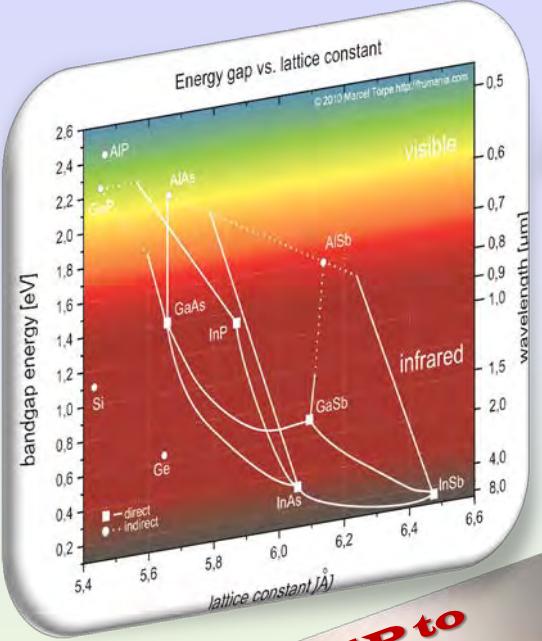
First Demonstration of QKD on GE-PON with simultaneous conventional data transmission

Growth Modelling



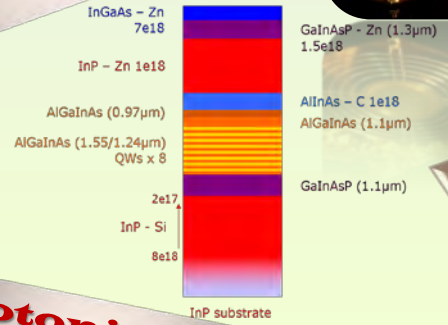
High purity materials

Metamorphic buffers and MOSFETs



Single QDs + non-classical light

From AlP to InSb

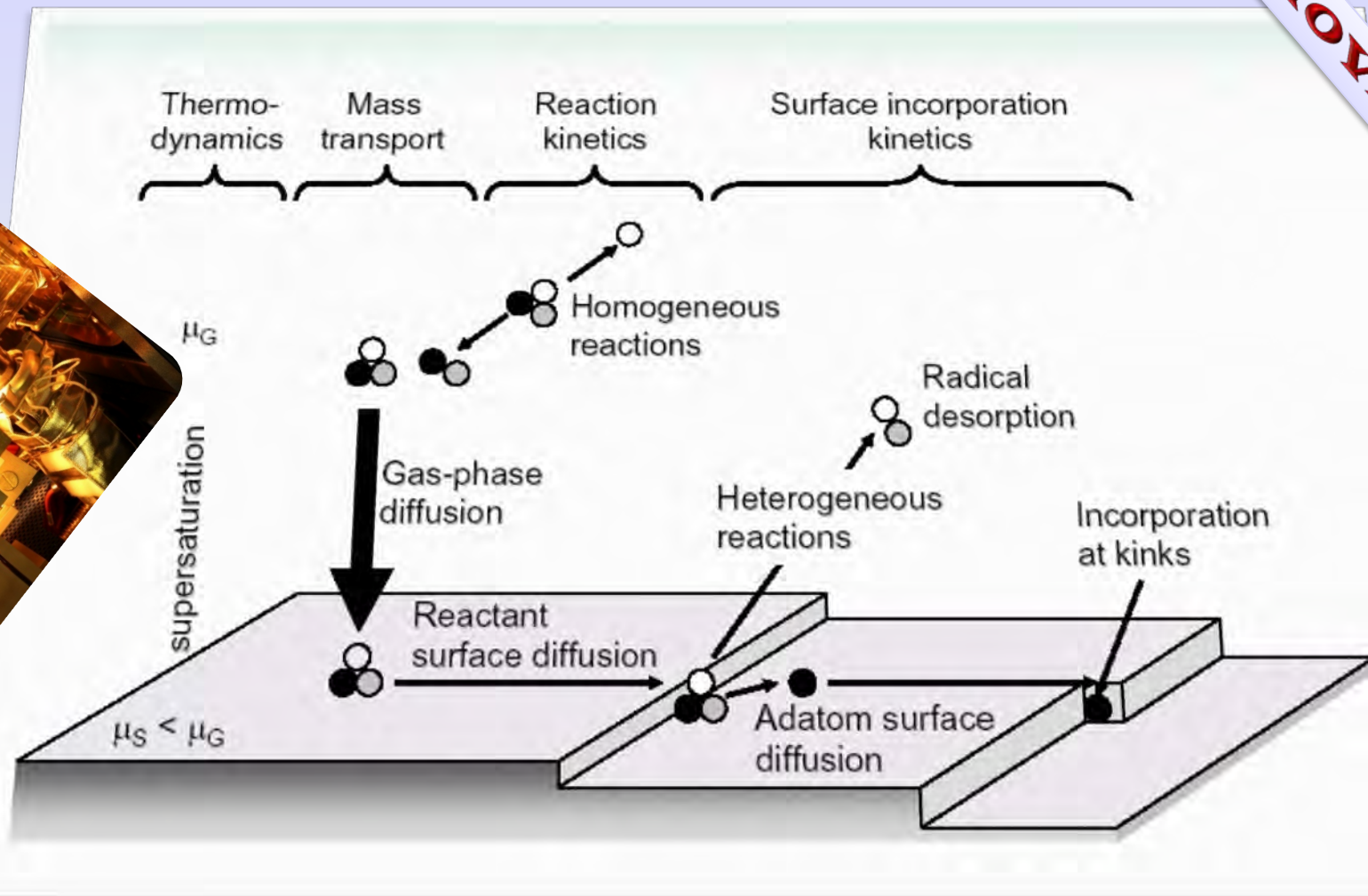
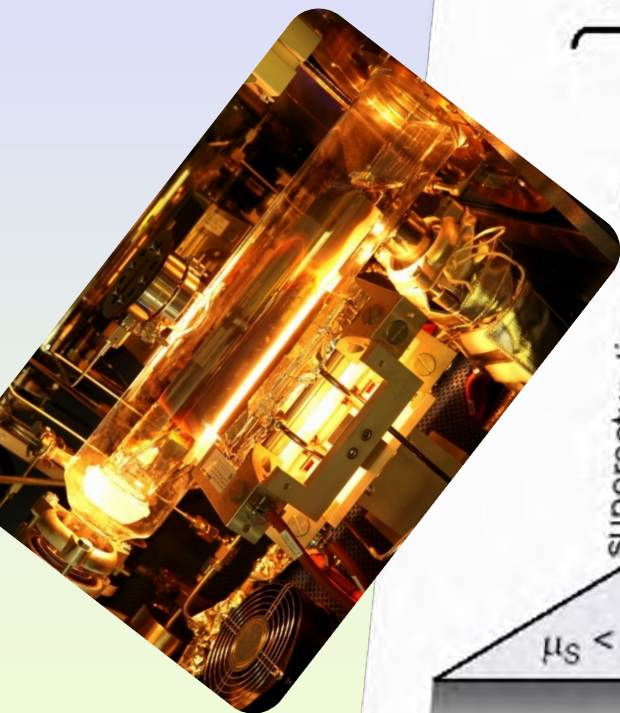


Photonic integration

Double reactor set-up: single wafer for high purity and 3x2inch for device growths

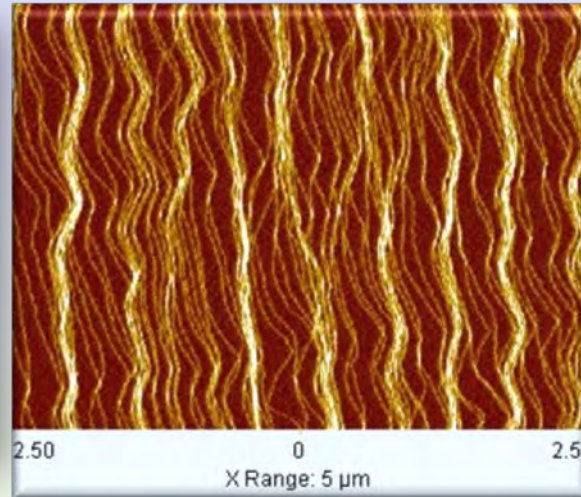
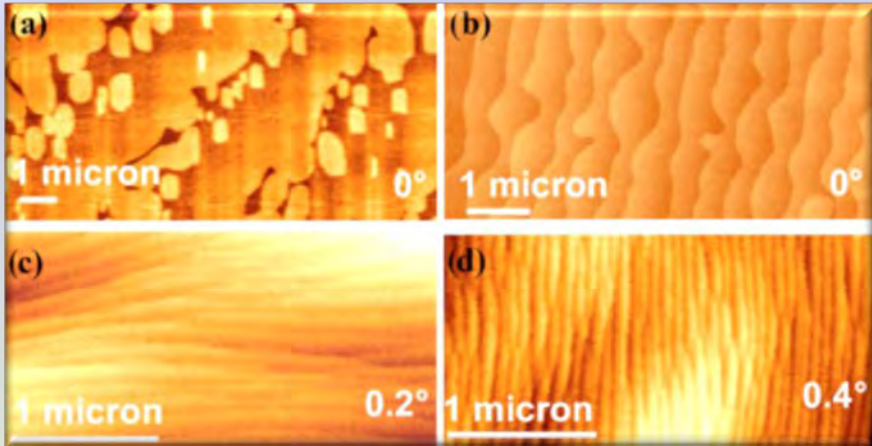
A quick reminder

MOYPE



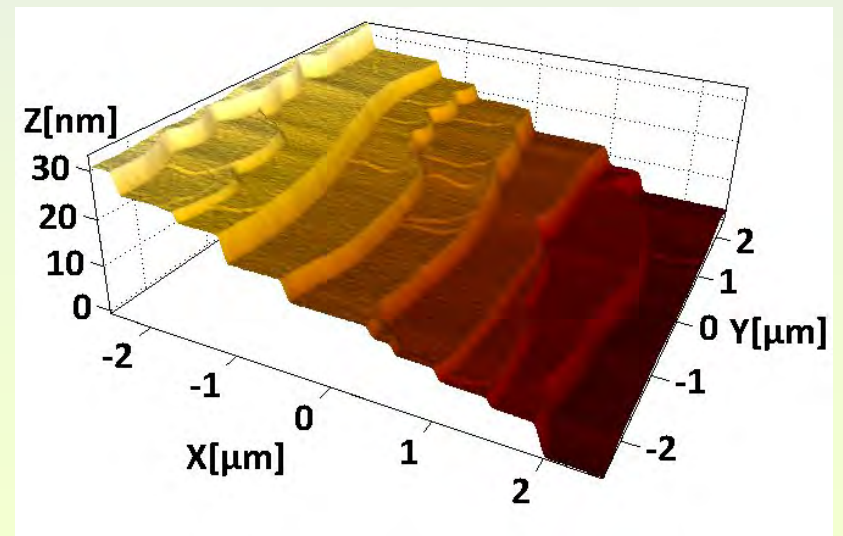
Surface organization

steps organise and evolve: step bunching, steps coalescence, periodic features....



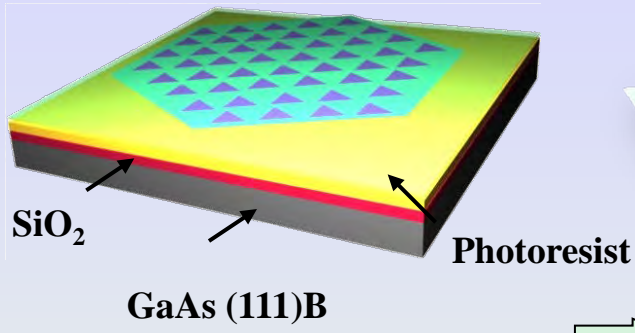
An example of InP (100) 0.4° A misorientation

GaAs (100) surfaces with different substrate miscut

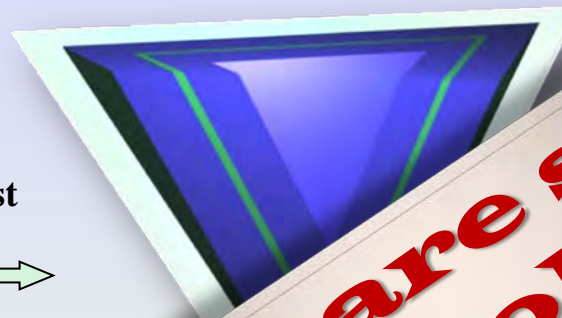


Our single quantum dots (which sometimes are actually decent “artificial atoms”.....)

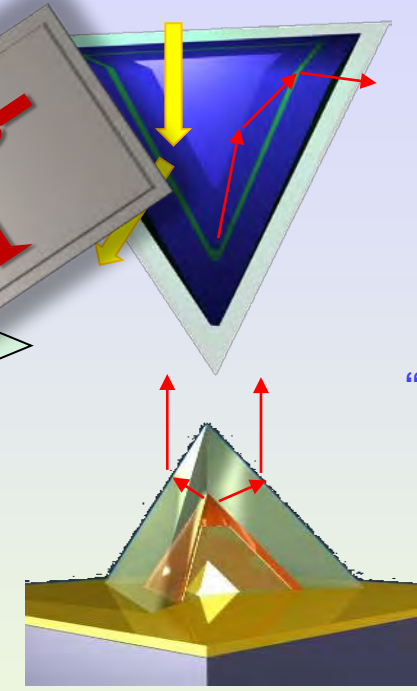
(111)B substrate patterning;
(photo)lithography+wet etching



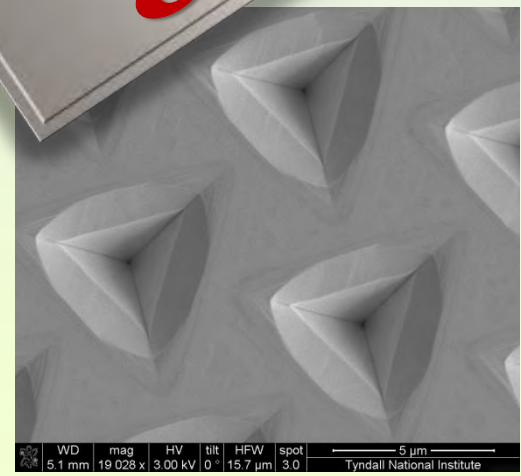
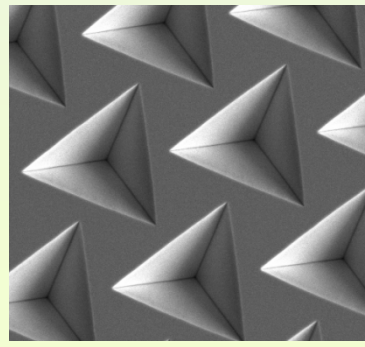
MOVPE growth:
QW like



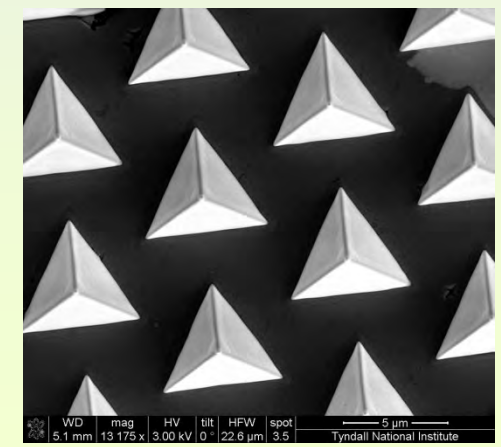
Post processing to enhance
extraction



they are site-controlled



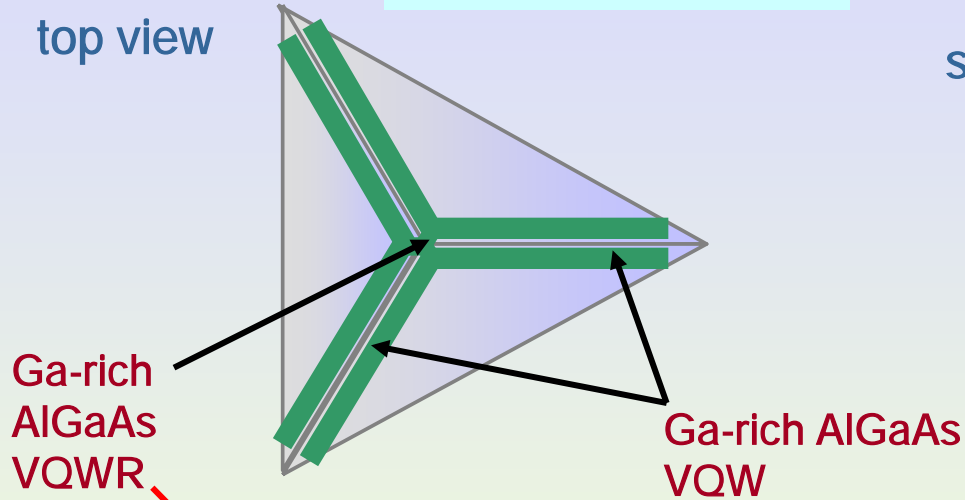
"apex up" or
"back etching",
prevents total
internal
reflection



System of interconnected nanostructures*

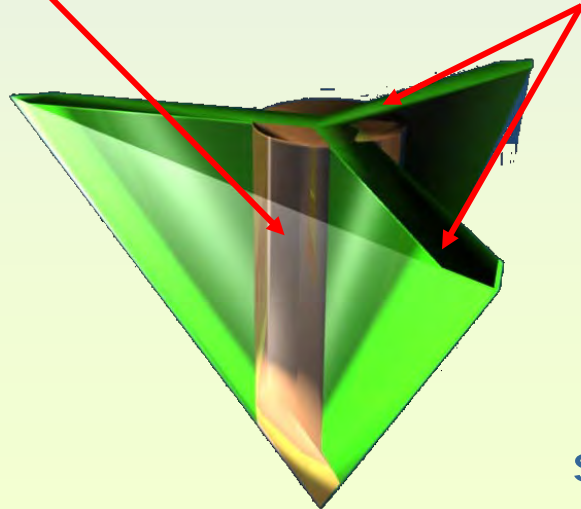
AlGaAs growth

top view



Ga-rich AlGaAs VQWR

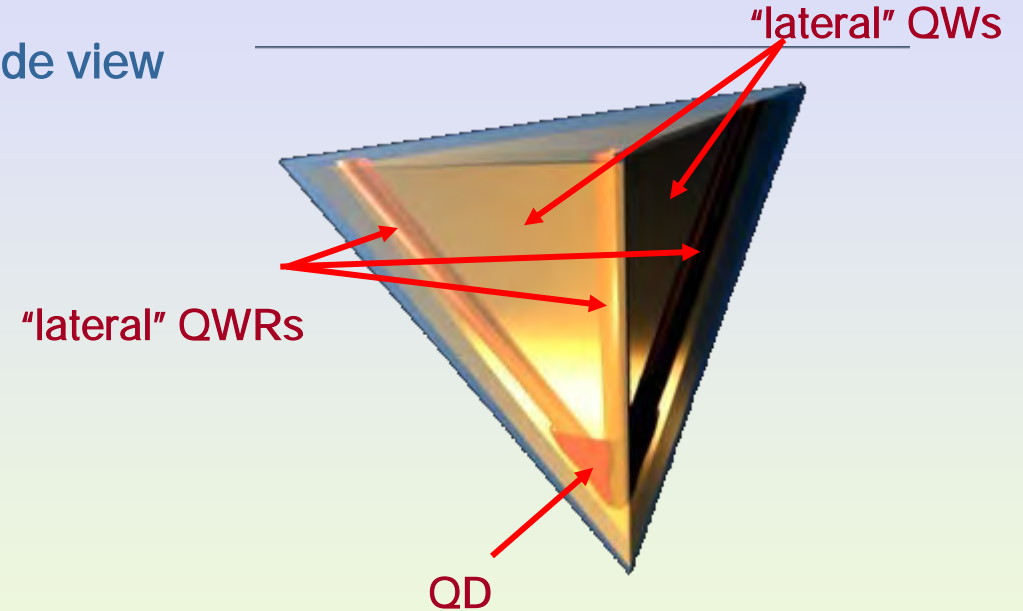
Ga-rich AlGaAs VQW



side view

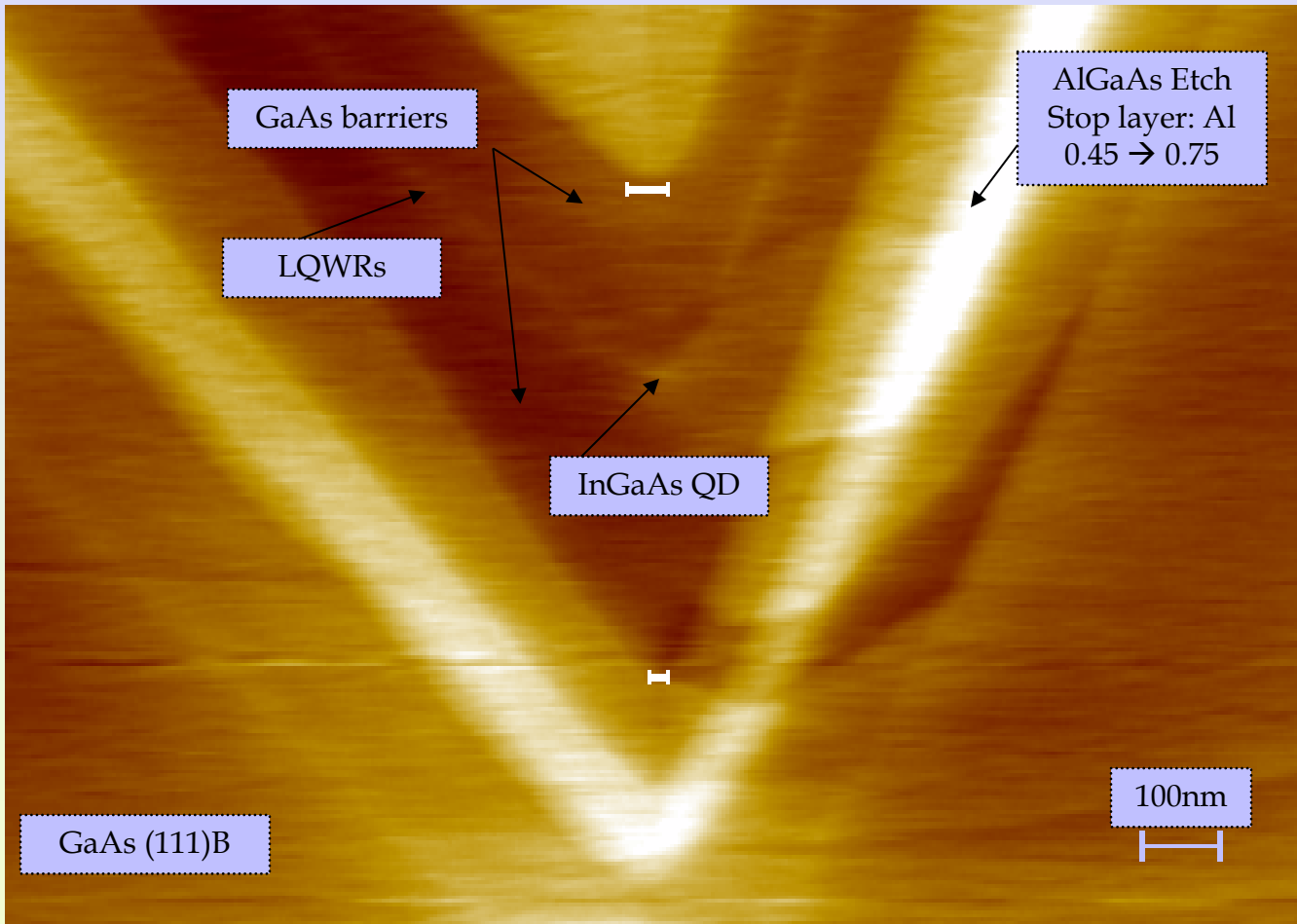
(In)GaAs growth

side view



QD

InGaAs dots in GaAs barriers...



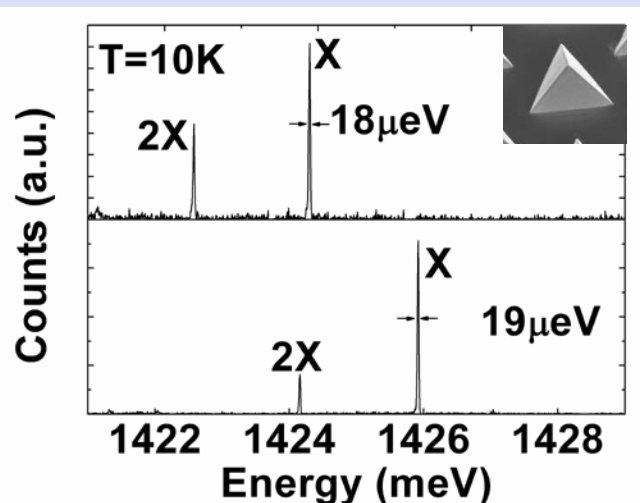
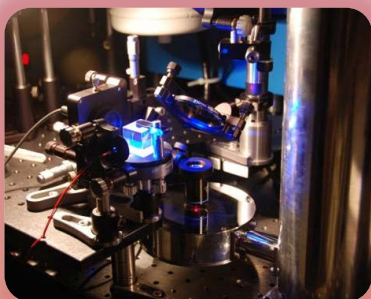
1.5 nm
 $\text{In}_{0.25}\text{Ga}_{0.75}\text{As}$ dot
in GaAs barriers

AFM cross section

Purity and uniformity (typically ~ 4 meV)...

Record linewidths for any site-controlled dots

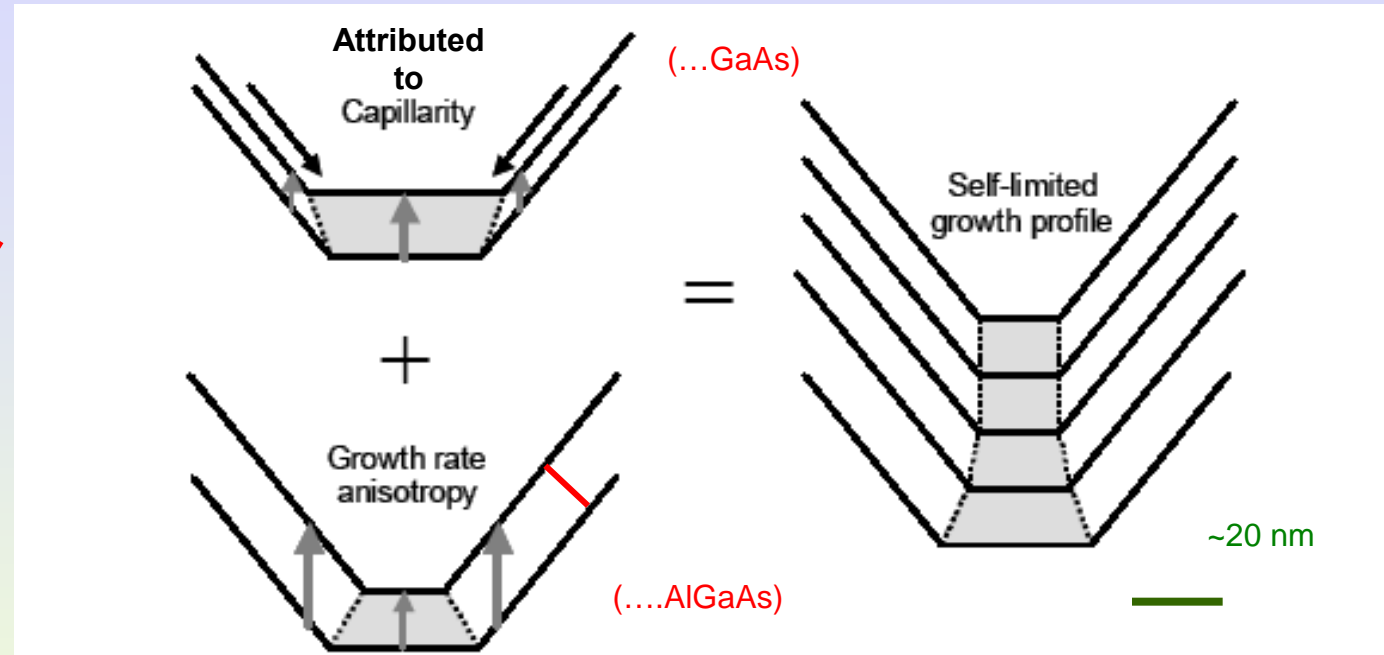
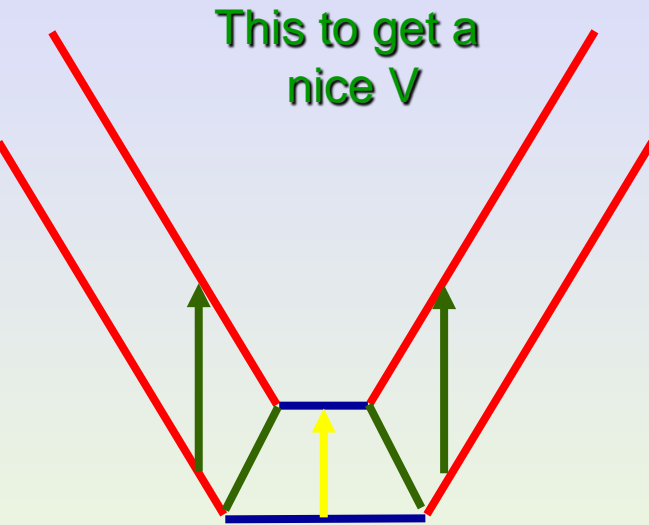
10 Kelvin!!!!



Best numbers to date, non resonant pumping, measured using interferometry: ~ 10 μeV

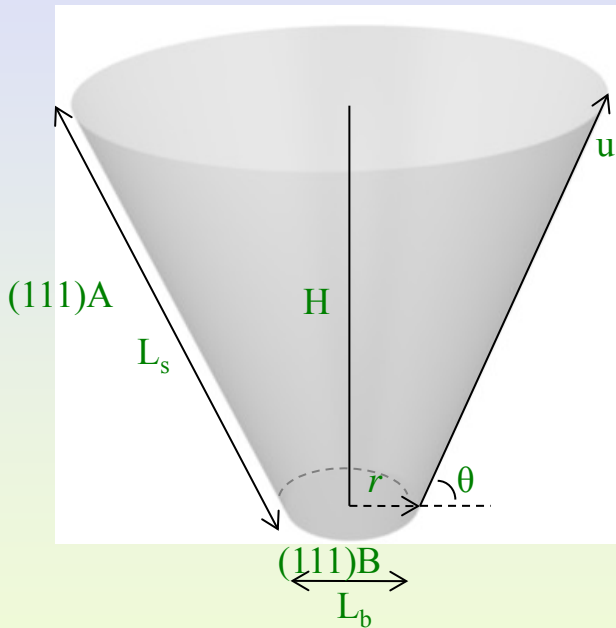
L.O. Mereni, V. Dimastrodonato, R.J. Young and E. Pelucchi, Appl. Phys. Lett. 94, 223121 (2009).

How they grow...like in V-grooves quantum wires....



Lateral growth rate much stronger than on bottom
Sidewalls grow faster...
So called capillarity..(but may be it is capillarity, may be not...)

In 3D... (similarly in 2D): it gives 2D diffusion, which one solves for stationary solution putting appropriate boundary conditions (111B/111A)



$$\nabla \cdot \mathbf{J}_i + F_i \delta_{\tau_i} \frac{n_i}{\tau_i} = 0, \quad \mathbf{J}_i = -D_i \nabla n_i$$

Decomposition rate anisotropy: $r = \frac{F_s}{F_b} > 1$

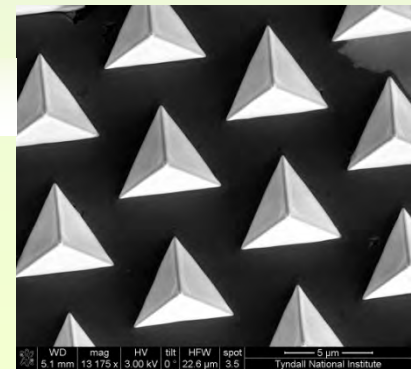
Surface diffusion (+ “capillarity”): $D_i = a^2 v \exp(-E_i^D/k_B T_G)$

Incorporation rate: $\tau_i = C_\tau \exp(E_i^\tau/k_B T_G)$

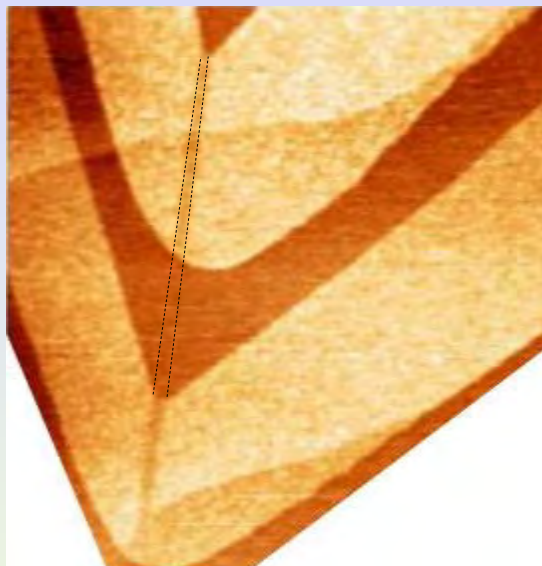
$$R_i = \frac{dz_i}{dt} = \Omega_0 \frac{n_i}{\tau_i}$$

Precursors decomposition only appear as an extra deposition flux, F...

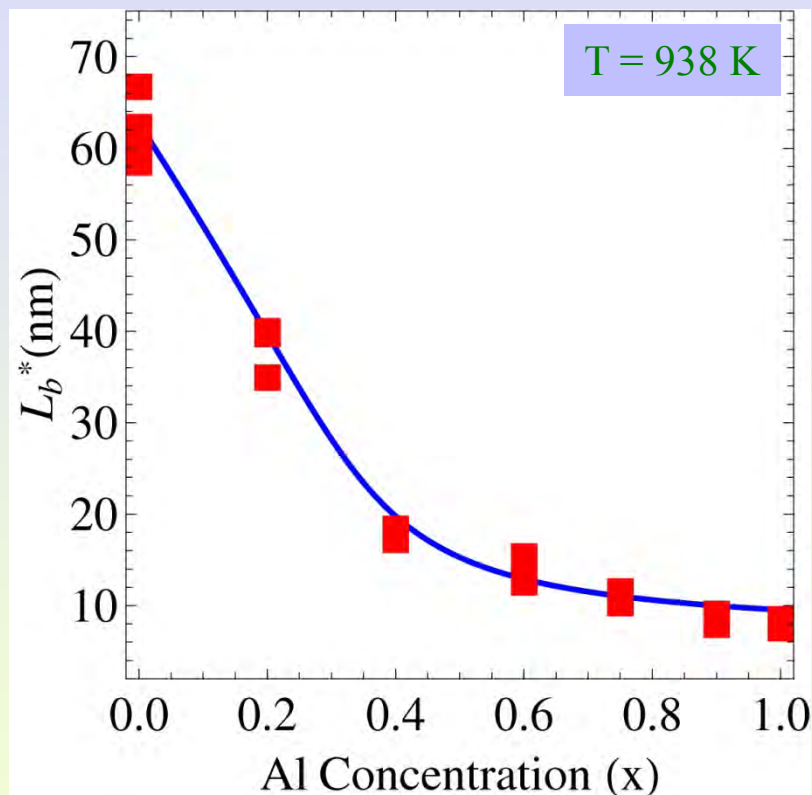
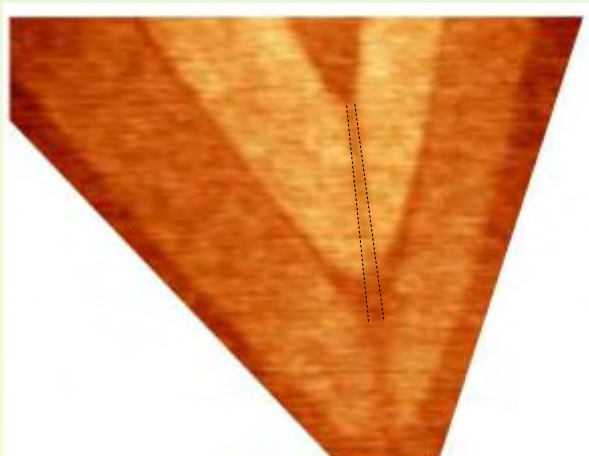
V. Dimastrodonato, E. Pelucchi, and D. D. Vvedensky, “Self-limiting profile evolution of seeded two- and three- dimensional nanostructures during metalorganic vapour-phase epitaxy”, Phys. Rev. Lett. 96, 130501 (2012).



Pyramids...self limited profile prediction
Note: much more difficult the VQWR concentration

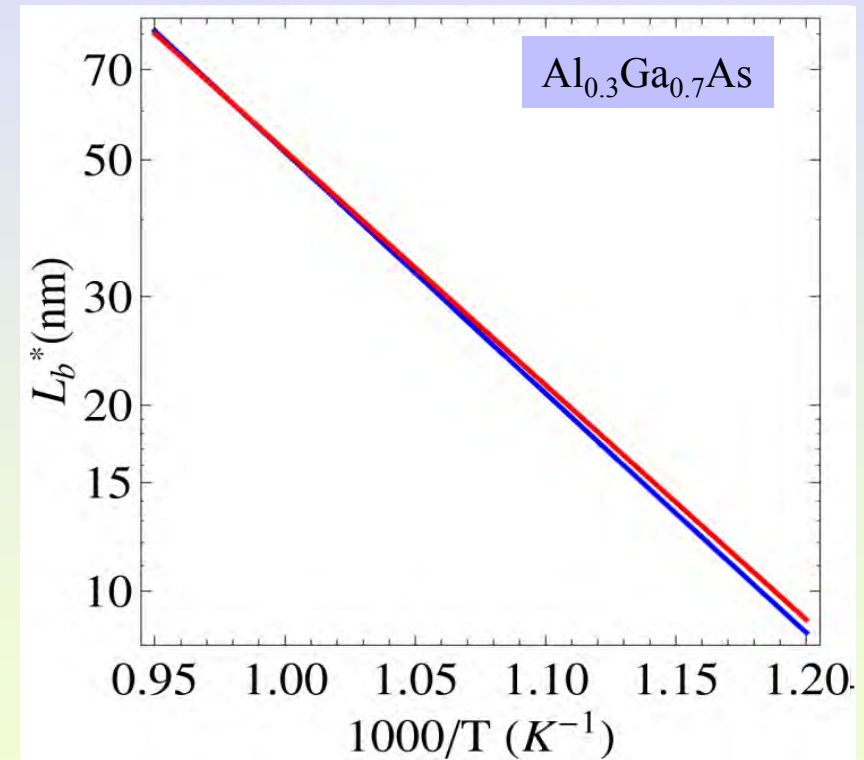
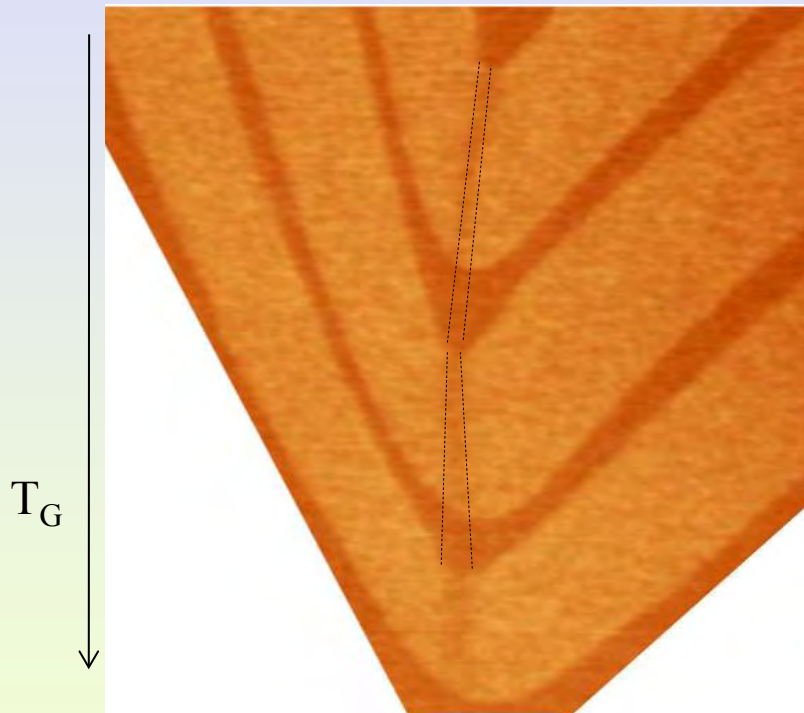


Al



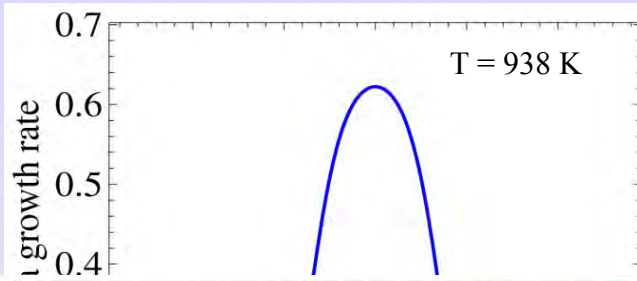
V. Dimastrodonato, E. Pelucchi, and D. D. Vvedensky, "Self-limiting profile evolution of seeded two- and three- dimensional nanostructures during metalorganic vapor-phase epitaxy", Phys. Rev. Lett. 96, 130501 (2012).

Self-limited regime: growth temperature

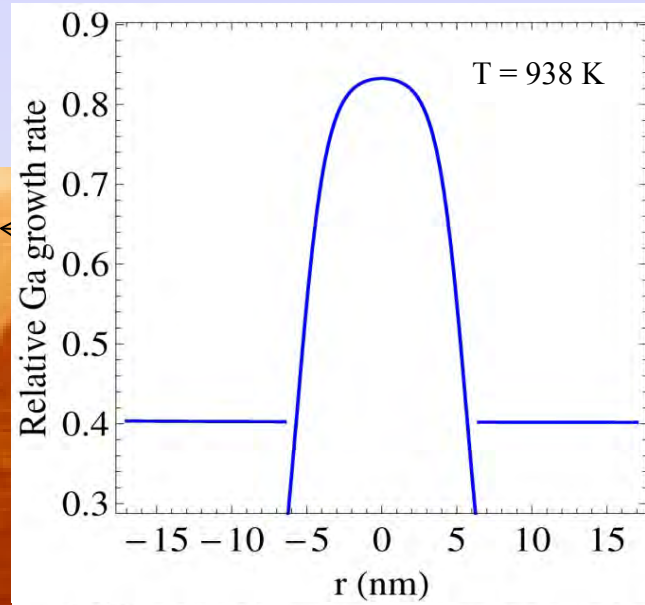


Self-limited regime: Ga segregation

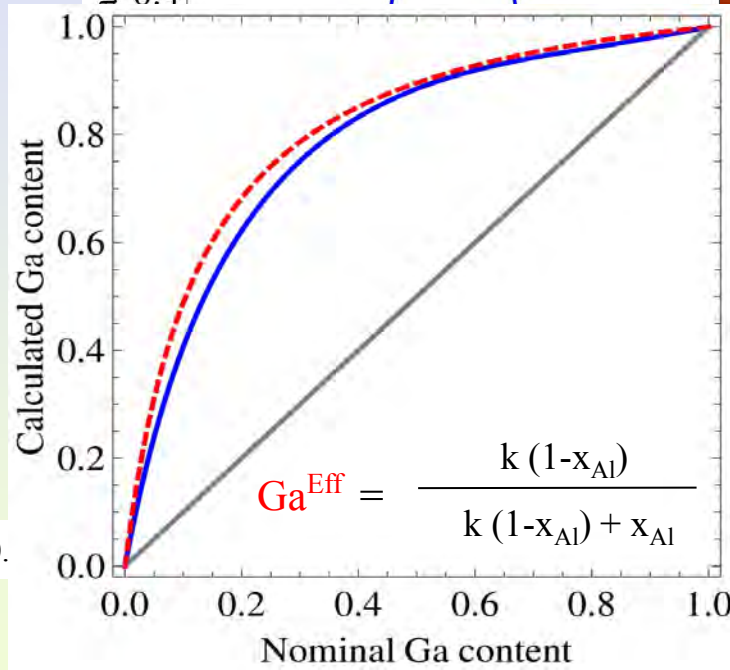
$Ga^{Nom} = 0.2$



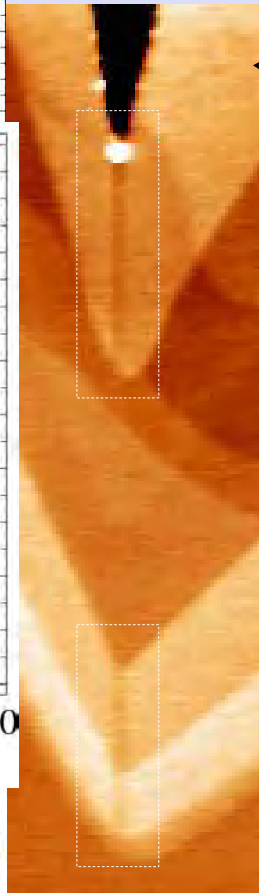
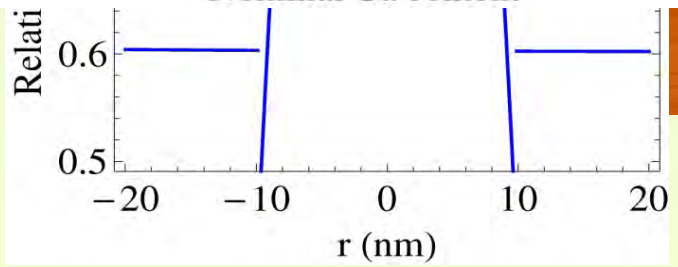
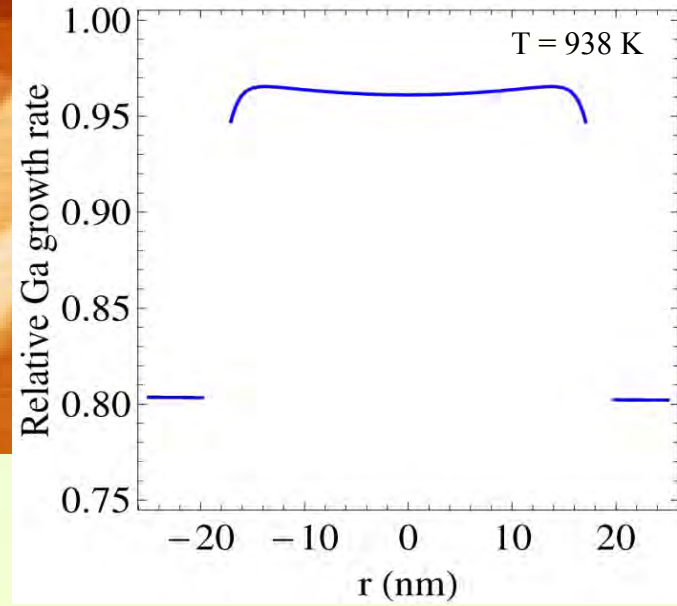
$Ga^{Nom} = 0.4$



$Ga^{Nom} = 0.$



$Ga^{Nom} = 0.8$



We can reproduce also InGaAs in V-grooves

Stefano Moroni et al., Journal of Applied Physics **117**, 164313 (2015).

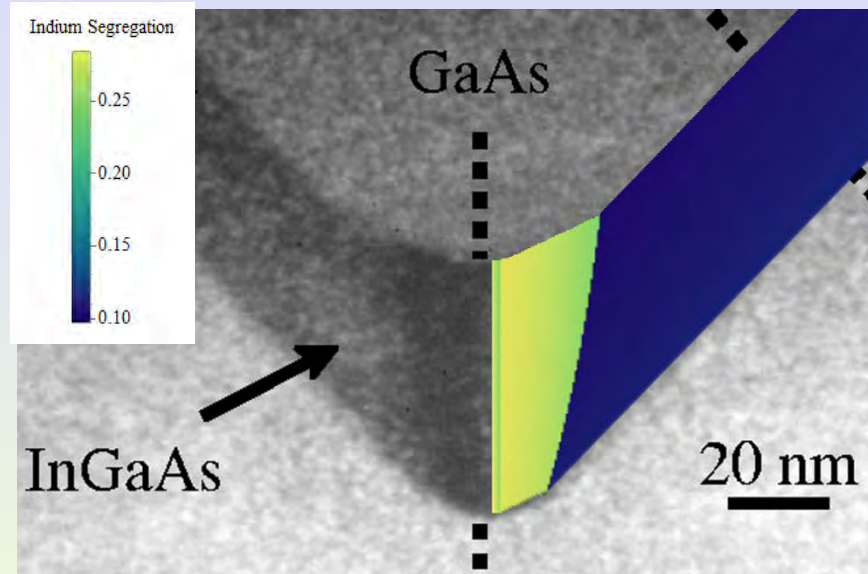


Fig. - Transient fit

Original figure from Lelarge et al., Applied Physics Letters **75**, 3300 (1999): only the TEM model is original

***Why it is not too bad to call QDs
artificial atoms....***

So, entangled photons....not our idea..since dots are “artificial atoms”...

One can use the transition from a “singlet state” (an “entangled” state because of indistinguishability, text book physics)

Just considering the two electrons

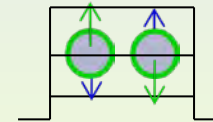
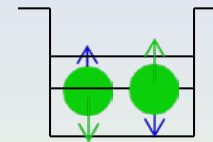
$$\frac{1}{\sqrt{2}}(|0\rangle|1\rangle - |1\rangle|0\rangle)$$

Two exchangeable electrons,
and two exchangeable holes...



appropriate parity under particle exchange

BiExcitonic State: 2X, two degenerate levels and Excitonic Singlet State



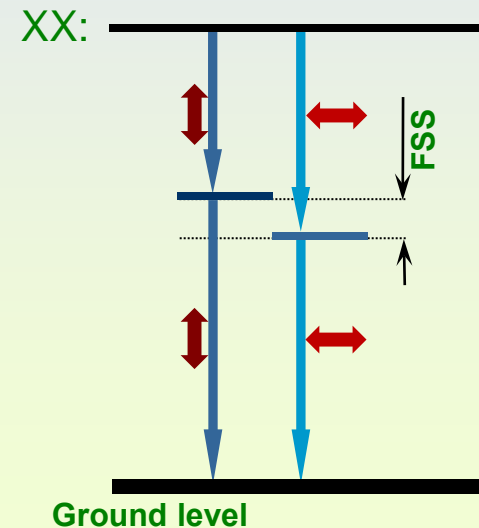
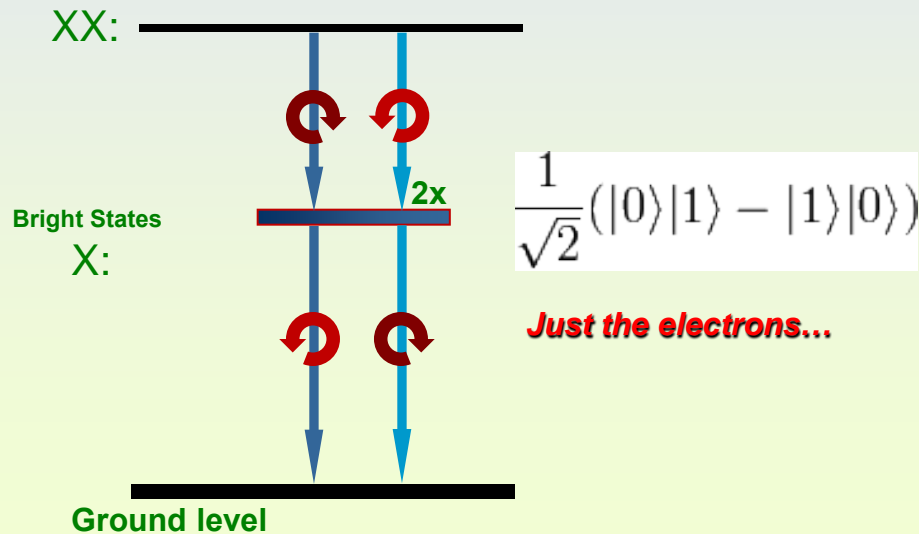
It has been done with real atoms in the early seventies..

$$|\psi\rangle = \frac{1}{\sqrt{2}}(|L_{XX}R_X\rangle + |R_{XX}L_X\rangle)$$

*It is clear from what I said that a biexciton (and not only one confined in a dot) is **not a separable state***

(D. A. Kleinman Phys. Rev. B 28, 871 (1983) and many more)

And... the which path information story....at the beginning the community sort of "were puzzled".. because of asymmetry: must be a which path information (the jargon used)



Long story short if you have FSS...

$$|\psi\rangle = \frac{1}{\sqrt{2}} \left(|HH\rangle + e^{i2\pi FSS\tau/h} |VV\rangle \right)$$

R. Mark Stevenson et al. Phys Rev. Lett. 101, 170501 (2008)

When a FSS splitting is present the state tomography procedure averages over several randomly distributed/emitted different entangled states, practically resulting in an apparent classical state..... one is left with a statistical mixture...

During the cascade and the “flying” period, it stays as an entangled state

Rigorously, and outside specialized scientific jargon, in each specific repetition of the experiment there is no “which path” information in the cascade process, as only after the first photon is measured, the superposition entangled state is projected onto a specific polarization and energetic state

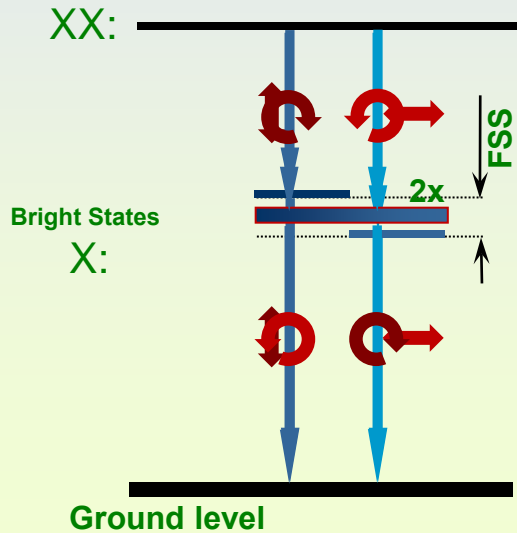
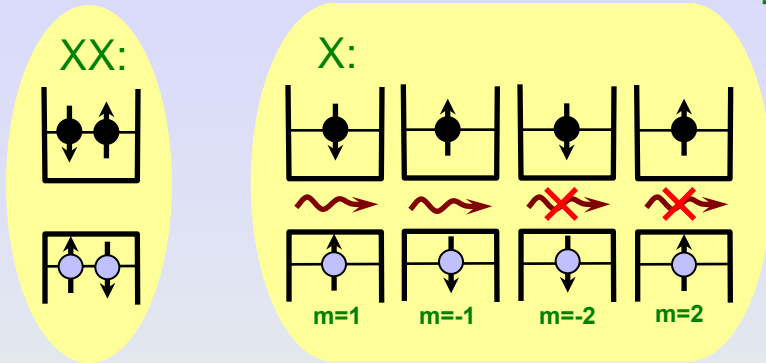
The process has, for this reason, no real similarity with a “double slit” experiment where the slit the photon has gone through is where a “which path” information obtained by some extra/external measurement can be effectively obtained. It would, on the other hand, have resemblances, **if any, with the phenomenon of coherence loss caused by random phases.** (ref. **M.O. Scully, B. Englert and H. Walter, Nature, 351, 6322 (1991)**)

So, long story short: it is easier with a symmetric dot to "see" the entanglement

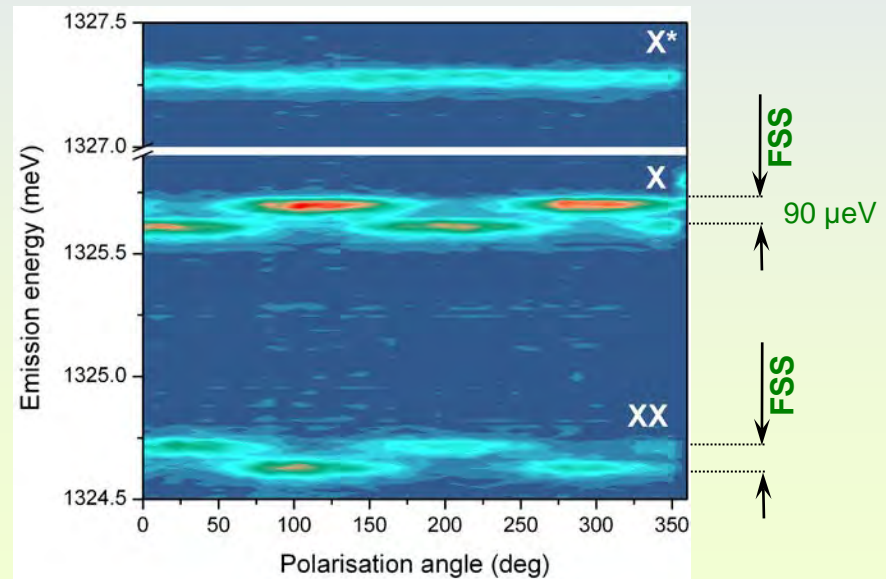
Pyramids should have C_{3V} symmetry which should ensure

suppression of the FSS.

- Singh, R., et al. Phys. Rev. Lett., 2009, 103(6),
- Schliwa, A., et al. Phys. Rev. B, 2009, 80(16),
- Karlsson, K.F., et al. Phys. Rev. B, 2010, 81(16).

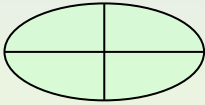
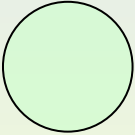
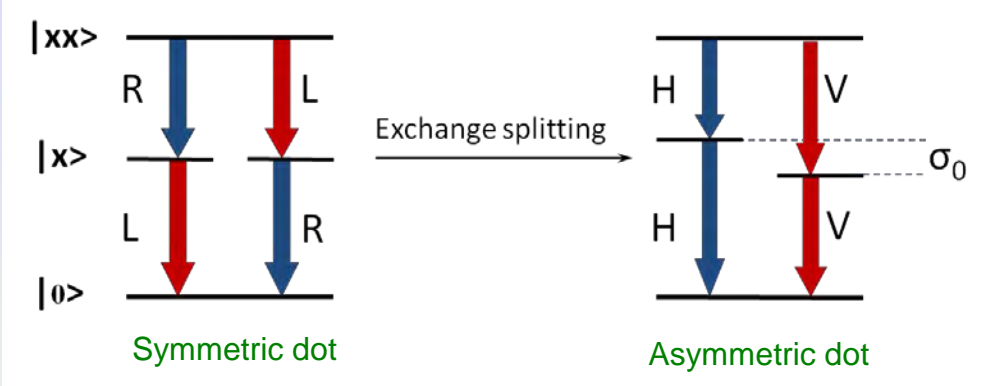
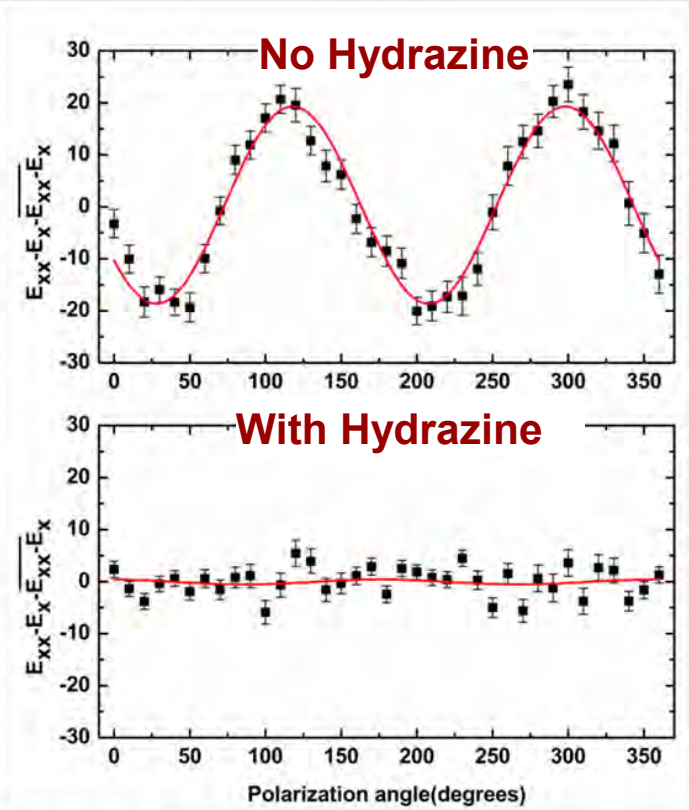


Low temperature grown, 1.2 nm InGaAsN QD:



$In_{0.25}Ga_{0.75}As_{1-\epsilon}N_{\epsilon}$...
some interesting unexpected features

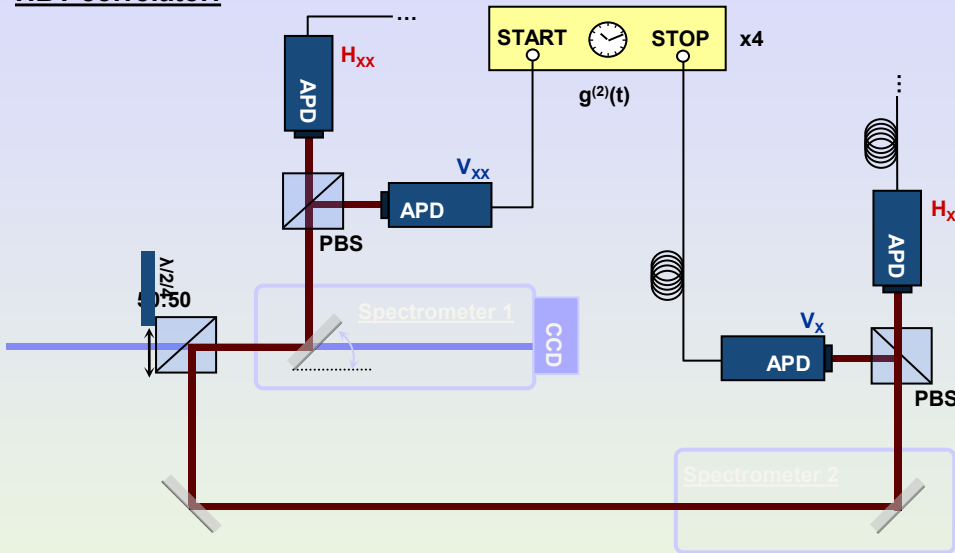
Measuring the fine structure splitting.... ..



This is unusual, we normally have some splitting (i.e. X and XX photons are linearly polarized.. not circularly polarized as they would be in a perfectly symmetric system)

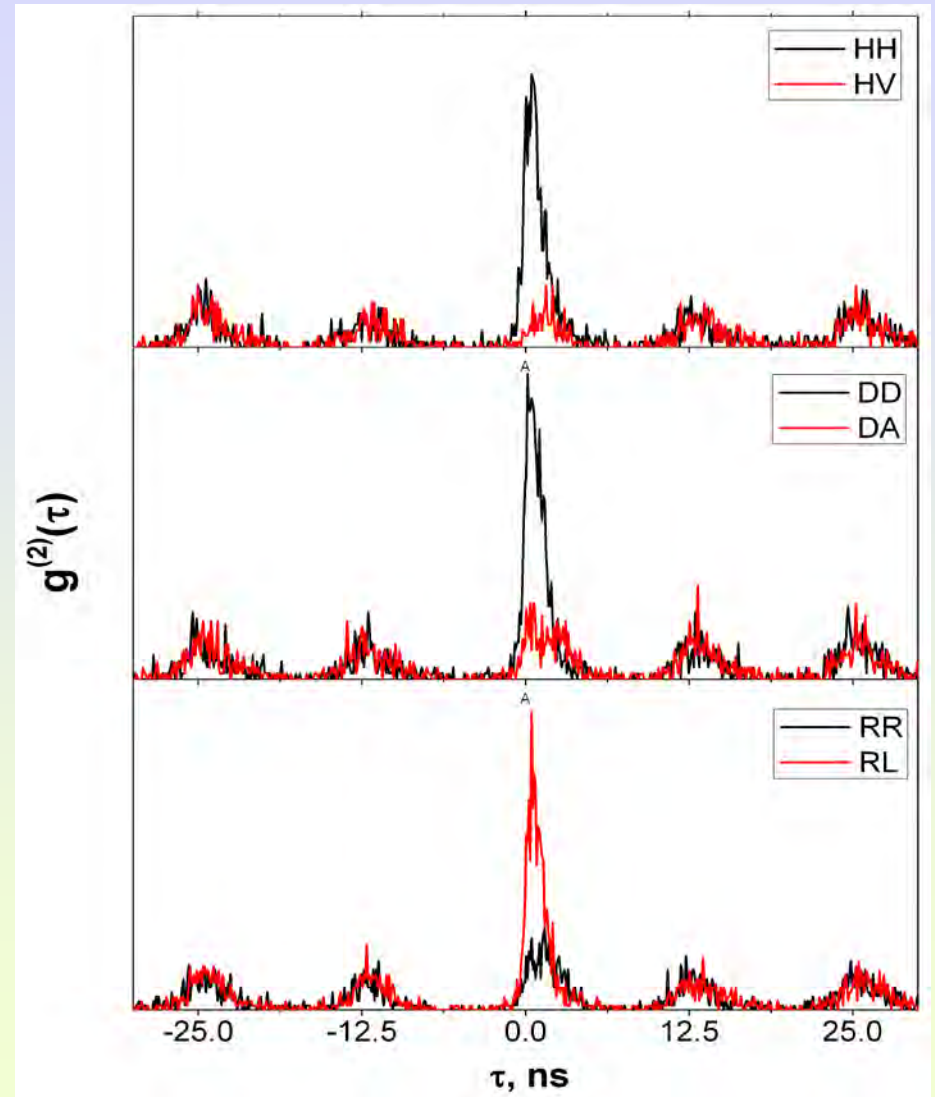
Difference in energy between the exciton and the biexciton for one dot plotted as a function of the half wave plate angle, in a standard InGaAs (no nitrogen) and $In_{0.25}Ga_{0.75}As_{1-\epsilon}N_{\epsilon}$ dots

HBT correlator:



$$\begin{aligned}
 |A\rangle &= \frac{1}{\sqrt{2}} (|H\rangle - |V\rangle) \\
 |D\rangle &= \frac{1}{\sqrt{2}} (|H\rangle + |V\rangle) \\
 |L\rangle &= \frac{1}{\sqrt{2}} (|H\rangle - i|V\rangle) \\
 |R\rangle &= \frac{1}{\sqrt{2}} (|H\rangle + i|V\rangle)
 \end{aligned}$$

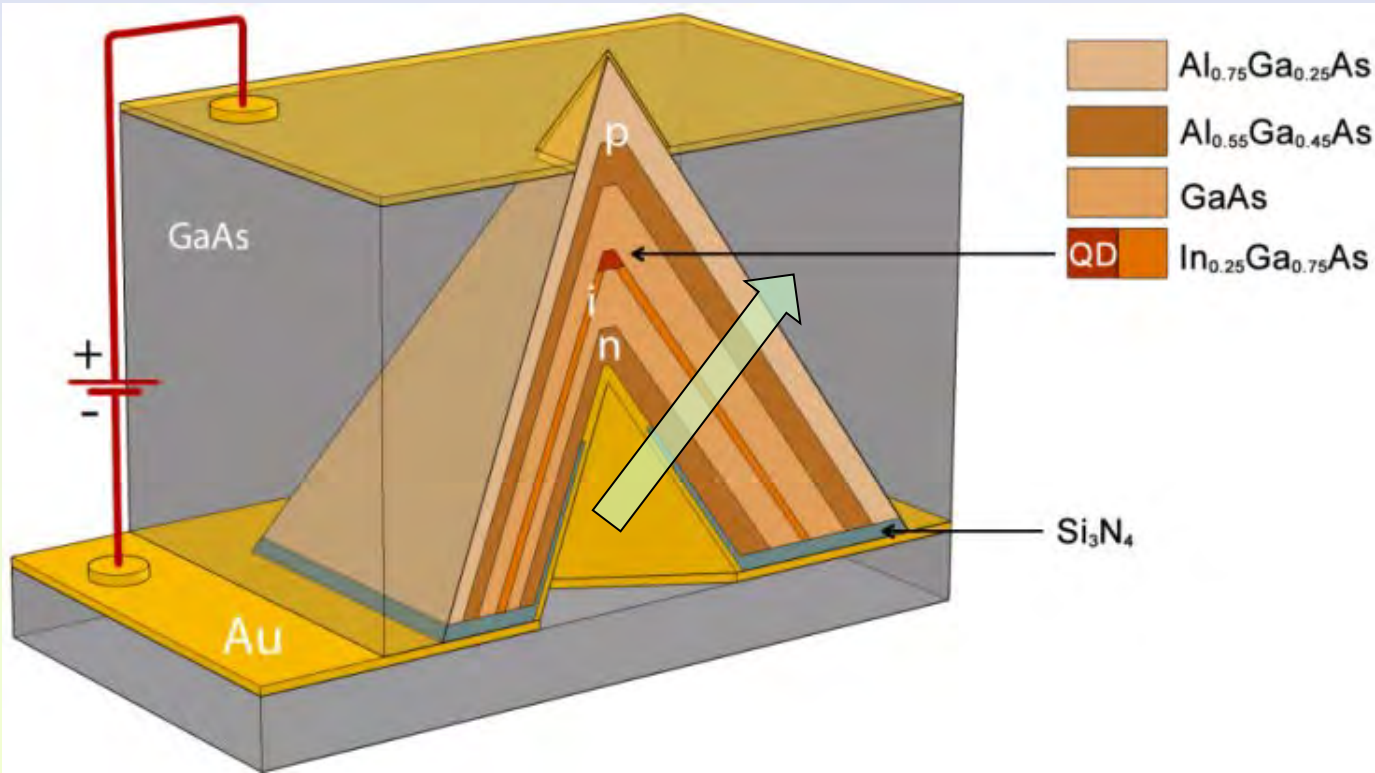
$$\begin{aligned}
 |\psi\rangle &= \frac{1}{\sqrt{2}} (|L_{xx}R_x\rangle + |R_{xx}L_x\rangle) = \\
 &= \frac{1}{\sqrt{2}} (|H_{xx}H_x\rangle + |V_{xx}V_x\rangle) = \\
 &= \frac{1}{\sqrt{2}} (|D_{xx}D_x\rangle + |A_{xx}A_x\rangle)
 \end{aligned}$$



G. Juska et al., Nature Photonics 7, 527, 2013

Can we electrically inject?

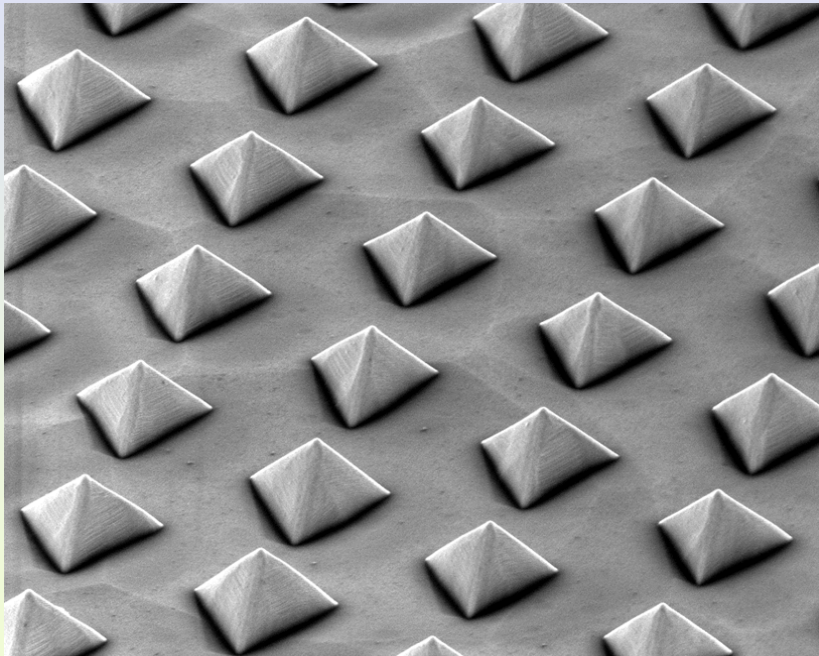
If you think about it, it should not work.....



Current prefers to go through the sides...shorter path (a factor of 3 or so!!!)..

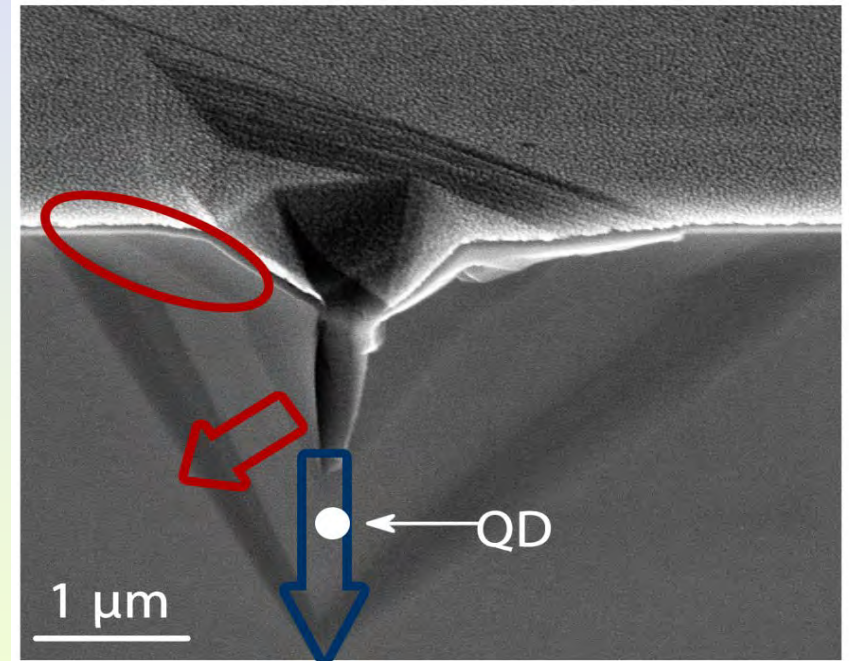
Device fabrication....issues

Apex-up geometry is essential to ensure high light extraction efficiency.

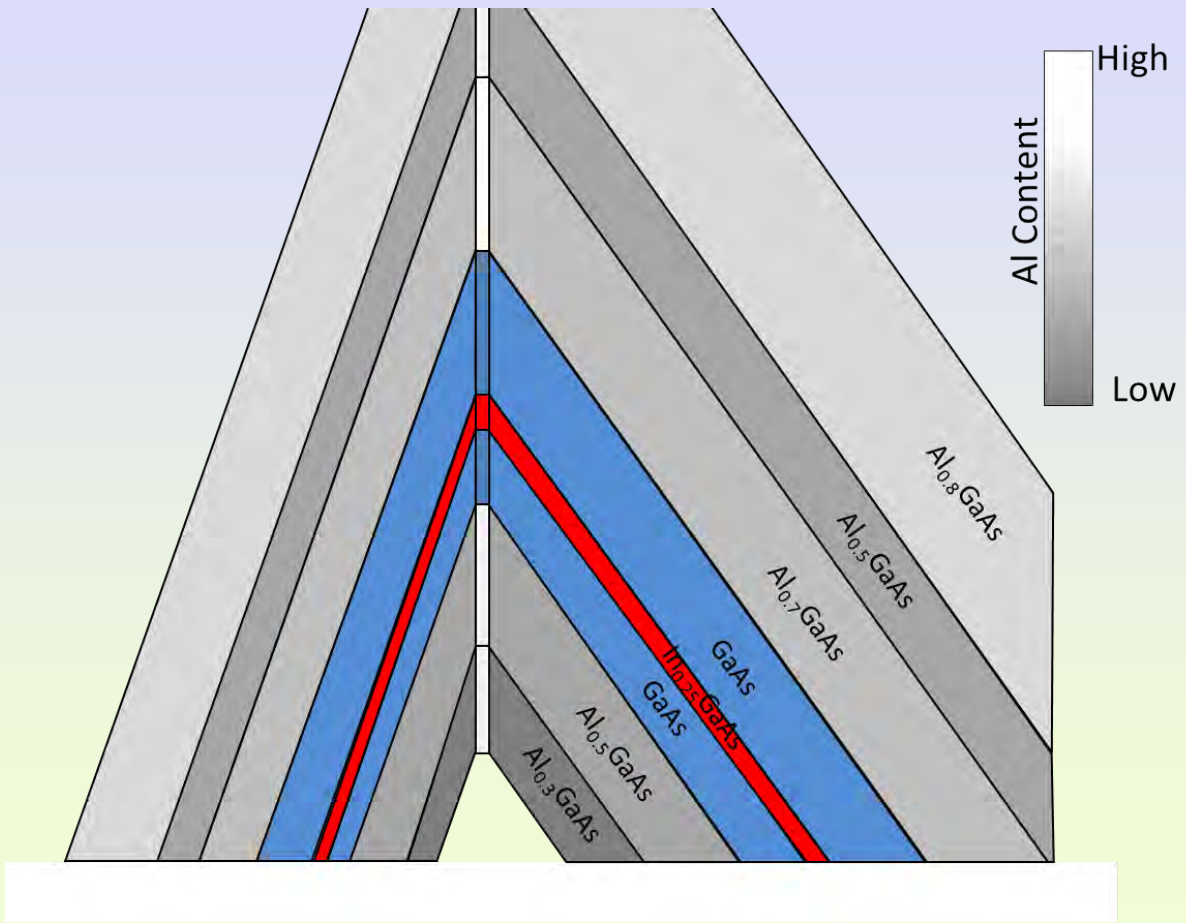
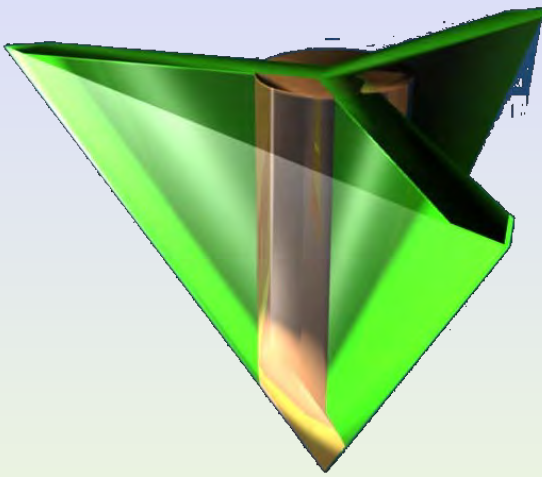


Issues:

- Non-planar structure
- Current leakage outside QD region



How to make it work... engineered injection... VQWR..

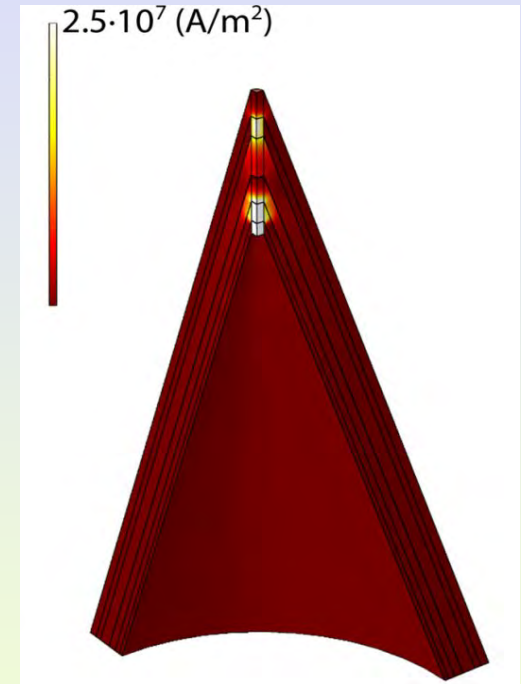
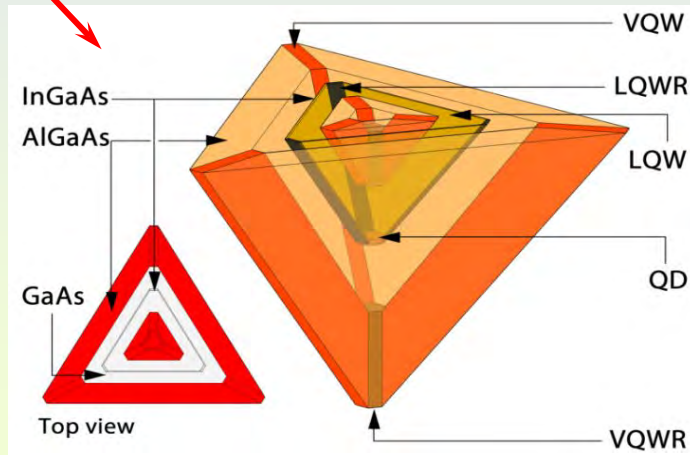


Selective injection of QDs

GaAs	10 nm	} n
Al _{0.3} GaAs	30	
Al _{0.75} GaAs	45	
GaAs	60	
In _{0.25} GaAs	0.55	} p
GaAs	90	
Al _{0.75} GaAs	45	
GaAs	60	
Al _{0.8} GaAs	90	} p
Al _{0.45-0.8} GaAs	45	
GaAs	40 nm	

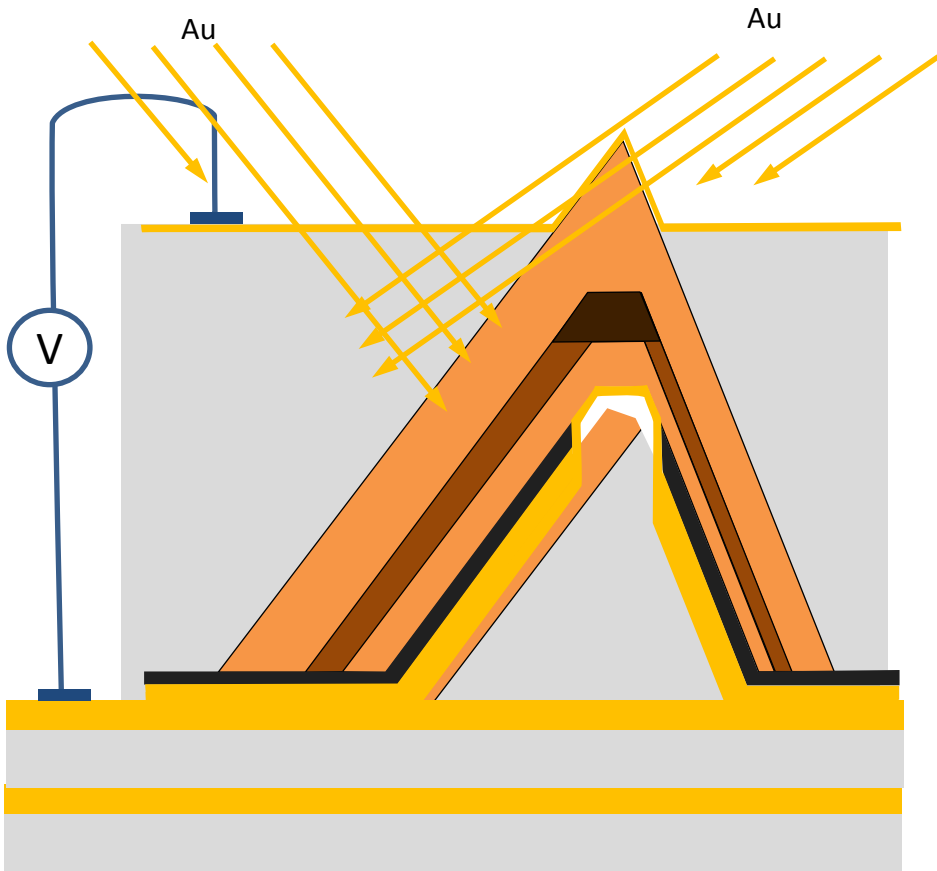


Vertical Quantum Wire (VQWR) – gallium segregated, self-formed nanostructure going along the center of a pyramid.

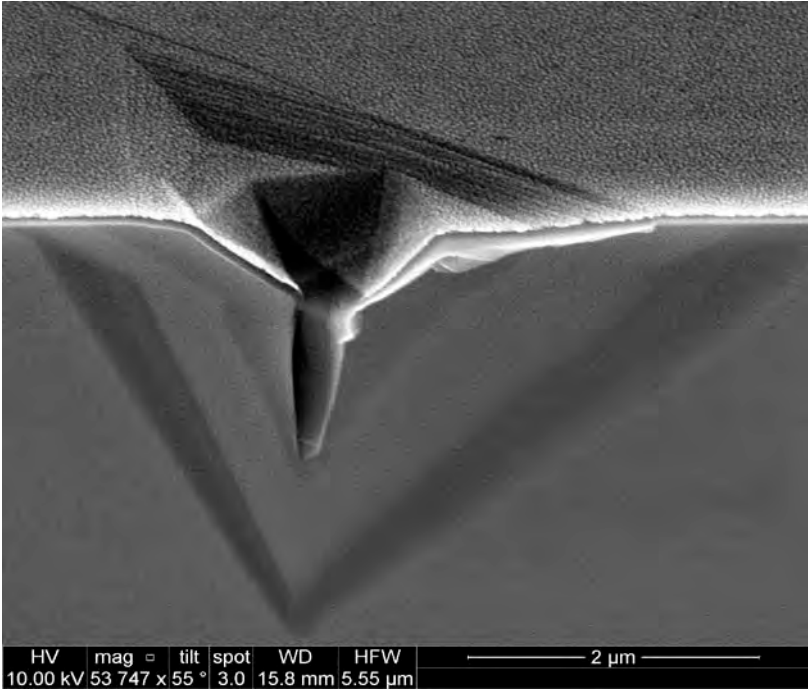


Simulation of current density distribution within the pyramid-like structure.

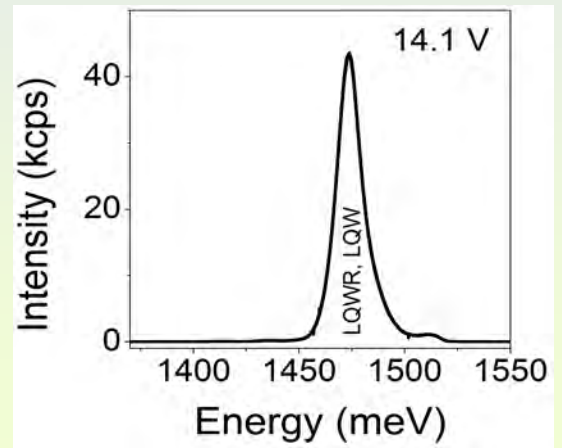
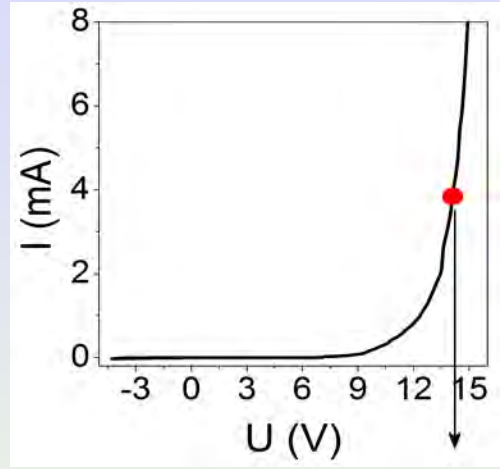
Diode processing



LED production steps:

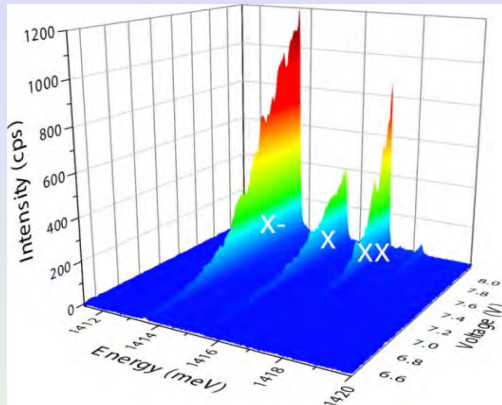


Electroluminescence

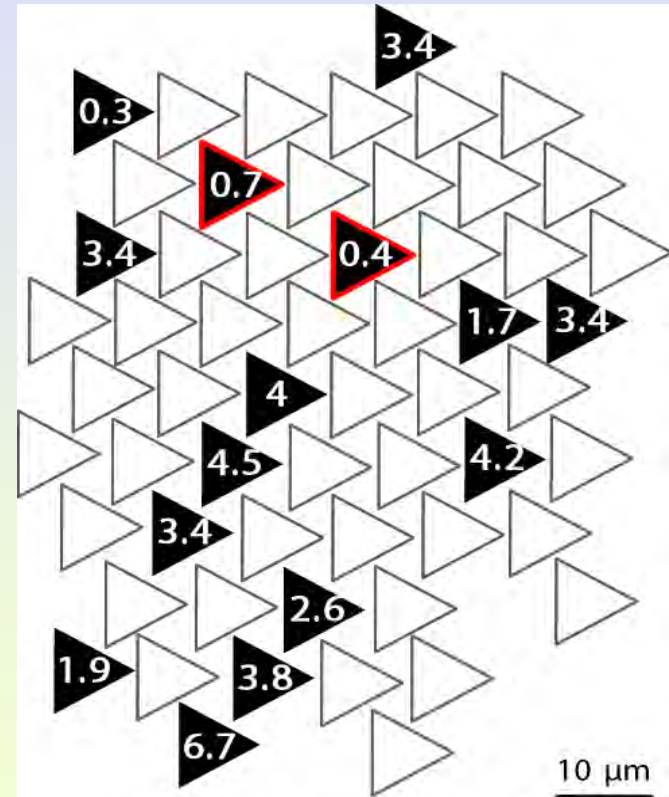


Symmetry

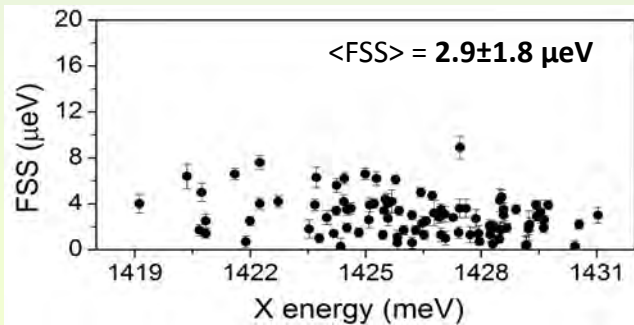
- A single QD electro-luminescence



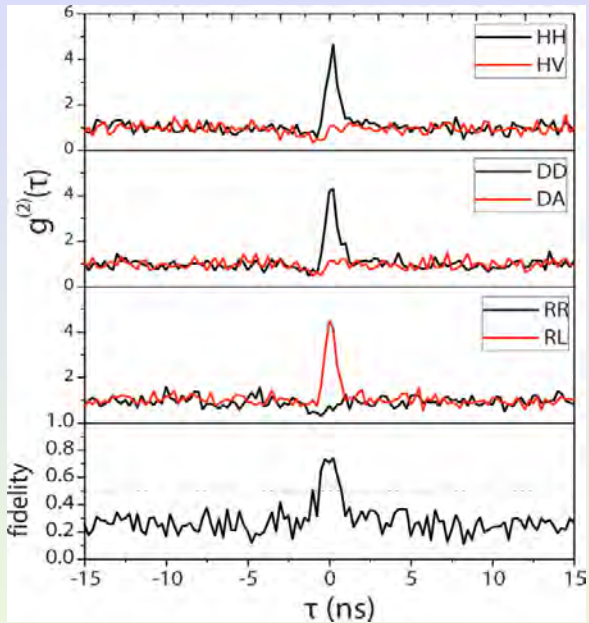
- Functional μ LED distribution and FSS values



- FSS values

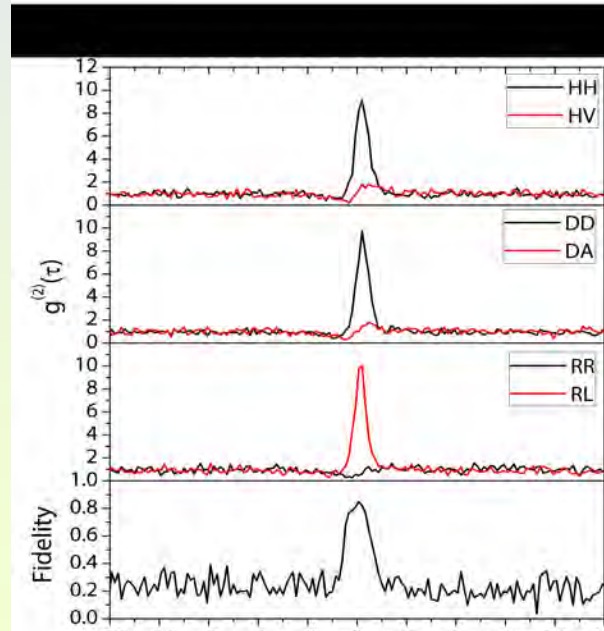
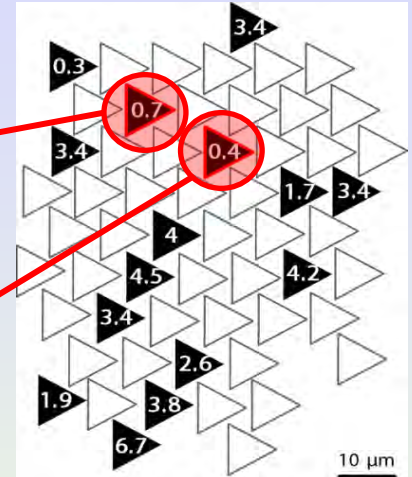


Entangled photon emission



$F = 0.69 \pm 0.06$

$F = 0.85 \pm 0.04$



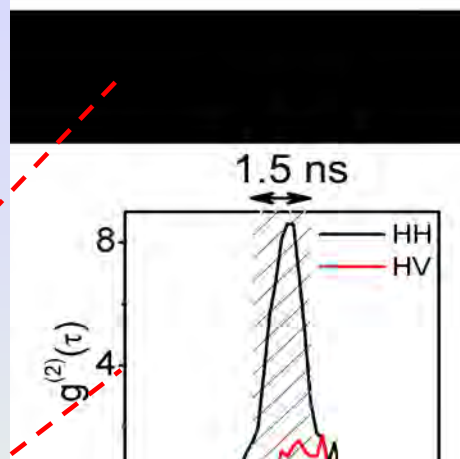
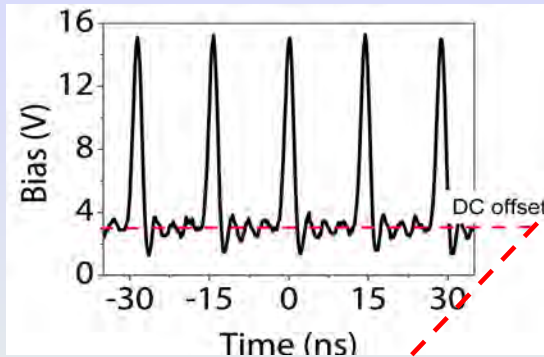
Fidelity of unpolarized source:

$$F = (1 + C_L + C_D - C_C)/4$$
 Degree of correlation:

$$C_{basis} = (g_{xx,x}^{(2)} - g_{xx,\bar{x}}^{(2)}) / (g_{xx,x}^{(2)} + g_{xx,\bar{x}}^{(2)})$$

Triggered entangled photon emission

- Pulsed injection:



- Simplified estimations of Bell's inequality:
(Young, R. J. PRL **102**, 030406, 2009)

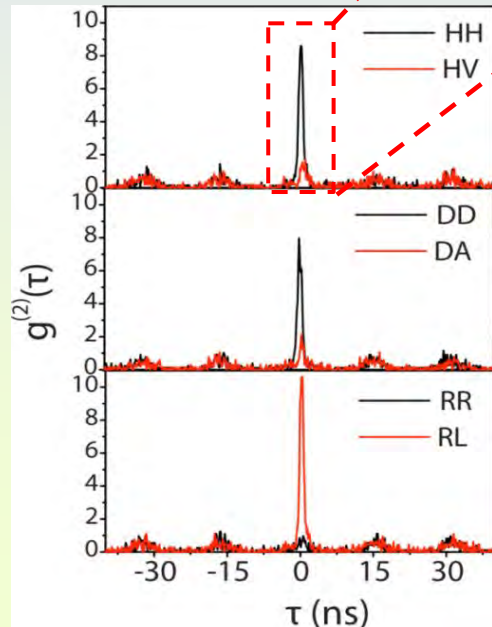
$$S_{RC} = \sqrt{2}(C_R - C_C) \leq 2$$

$$S_{RD} = \sqrt{2}(C_R + C_D) \leq 2$$

$$S_{DC} = \sqrt{2}(C_D - C_C) \leq 2$$

$$C_{basis} = (g_{xx,x}^{(2)} - g_{xx,\bar{x}}^{(2)}) / (g_{xx,x}^{(2)} + g_{xx,\bar{x}}^{(2)})$$

- Correlations:

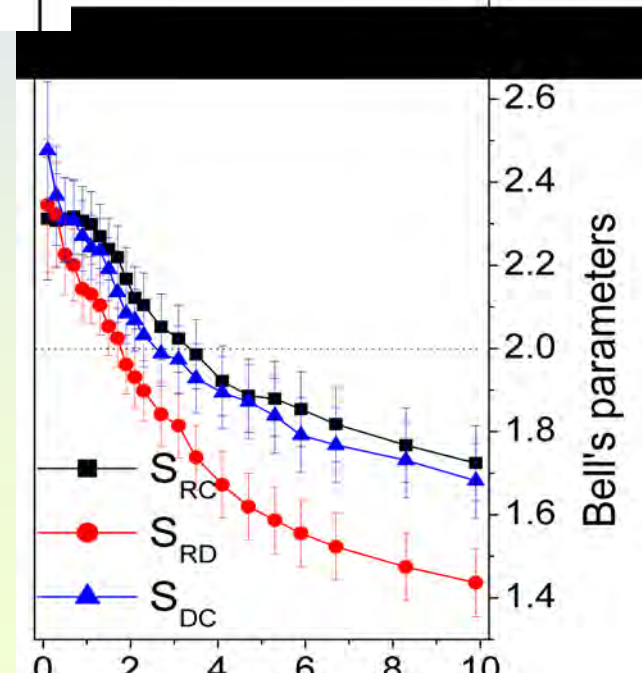


With 1.5 ns window and
75% intensity preserved:

$$S_{RD} = 2.053 \pm 0.070$$

$$S_{DC} = 2.191 \pm 0.075$$

$$S_{RC} = 2.239 \pm 0.074$$

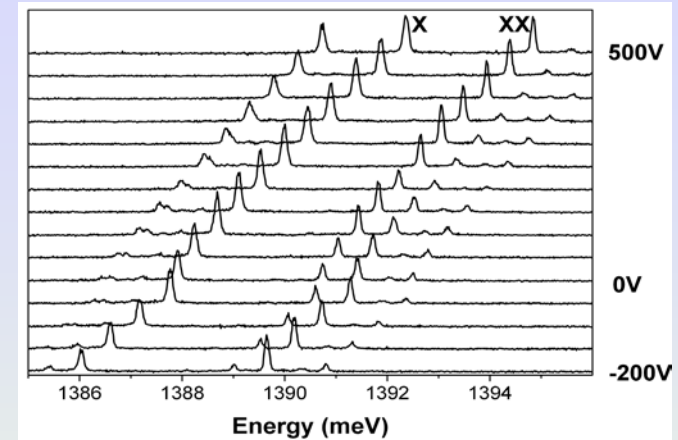


Short term future

Integration of QDs on piezoelectric actuators:

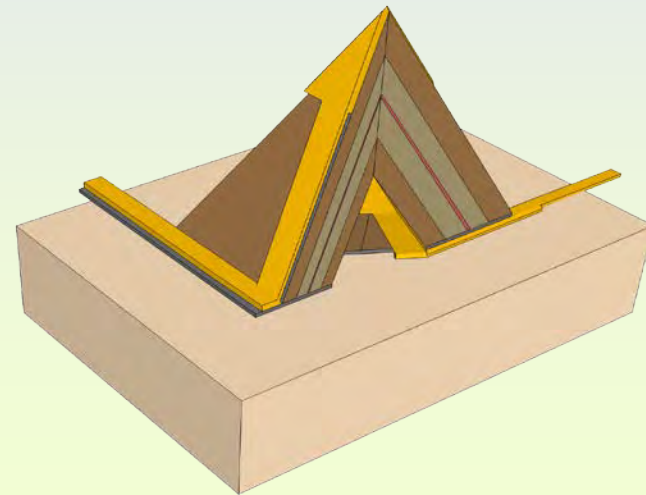
- Tuning emission energy.
- Tuning the fine-structure splitting.

Collaboration with JKU Linz (A. Rastelli, R. Trotta, et al.)



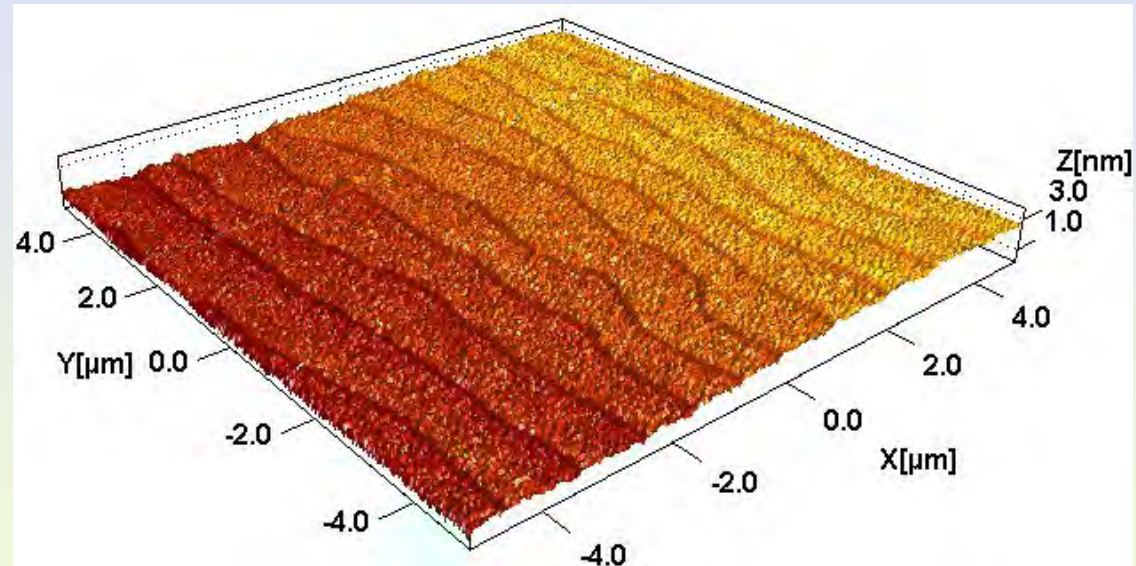
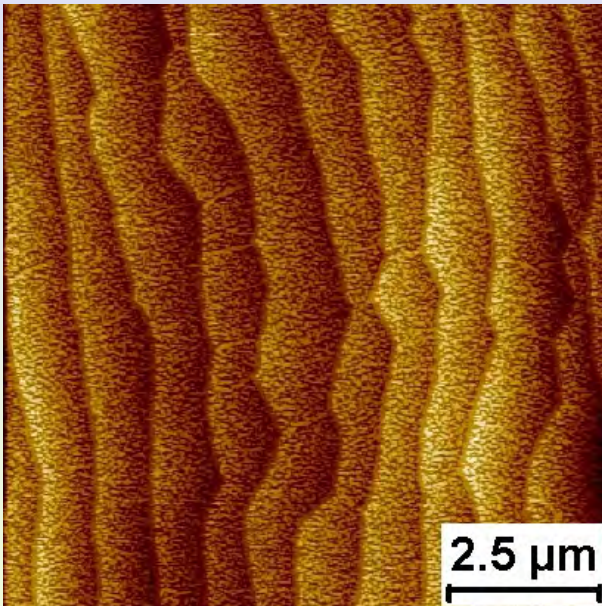
Adding local metallic contacts:

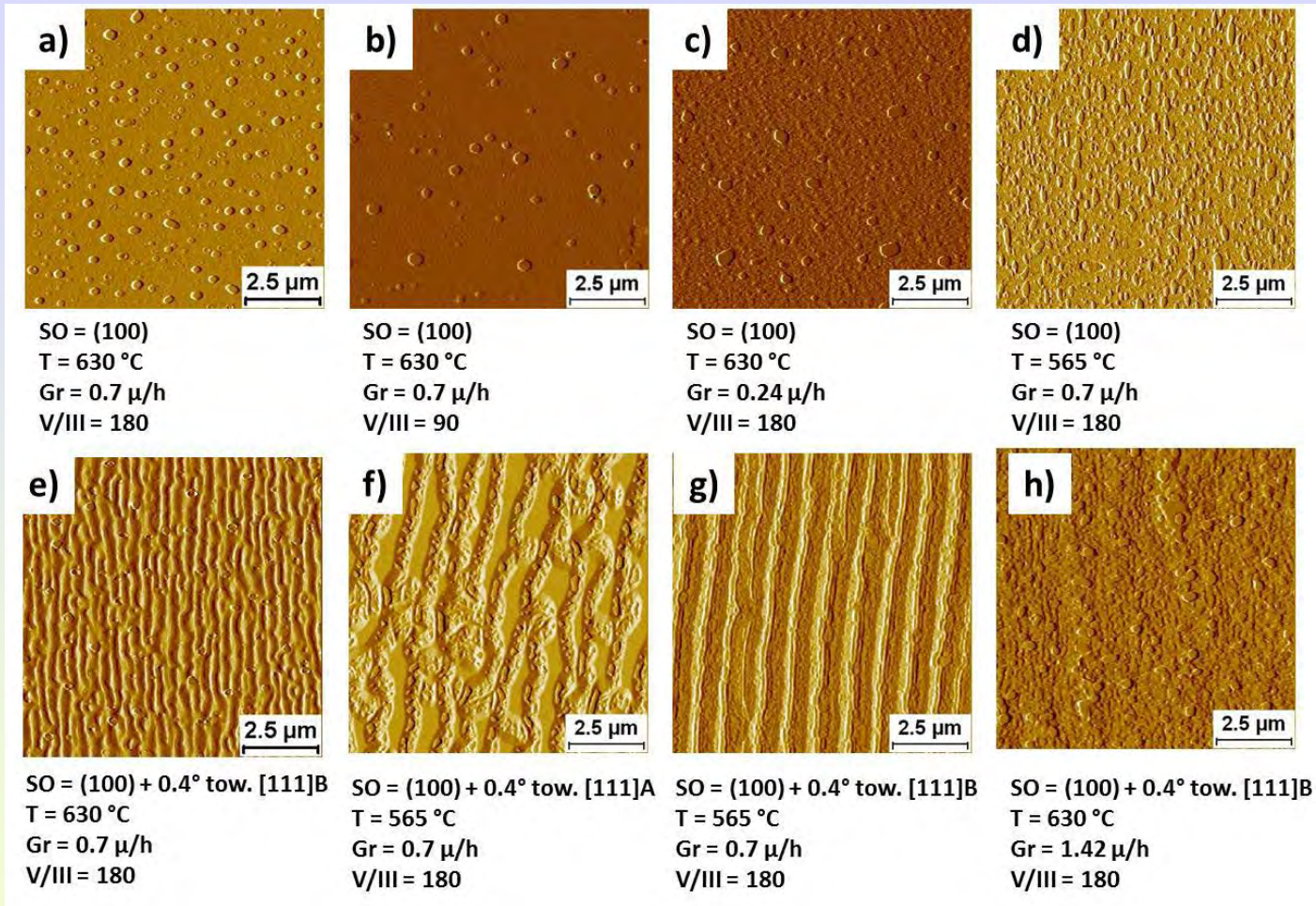
- Electric injection of carriers.
- Tuning emission energy.
- Tuning the fine-structure splitting.
- Electrical manipulation of spins.



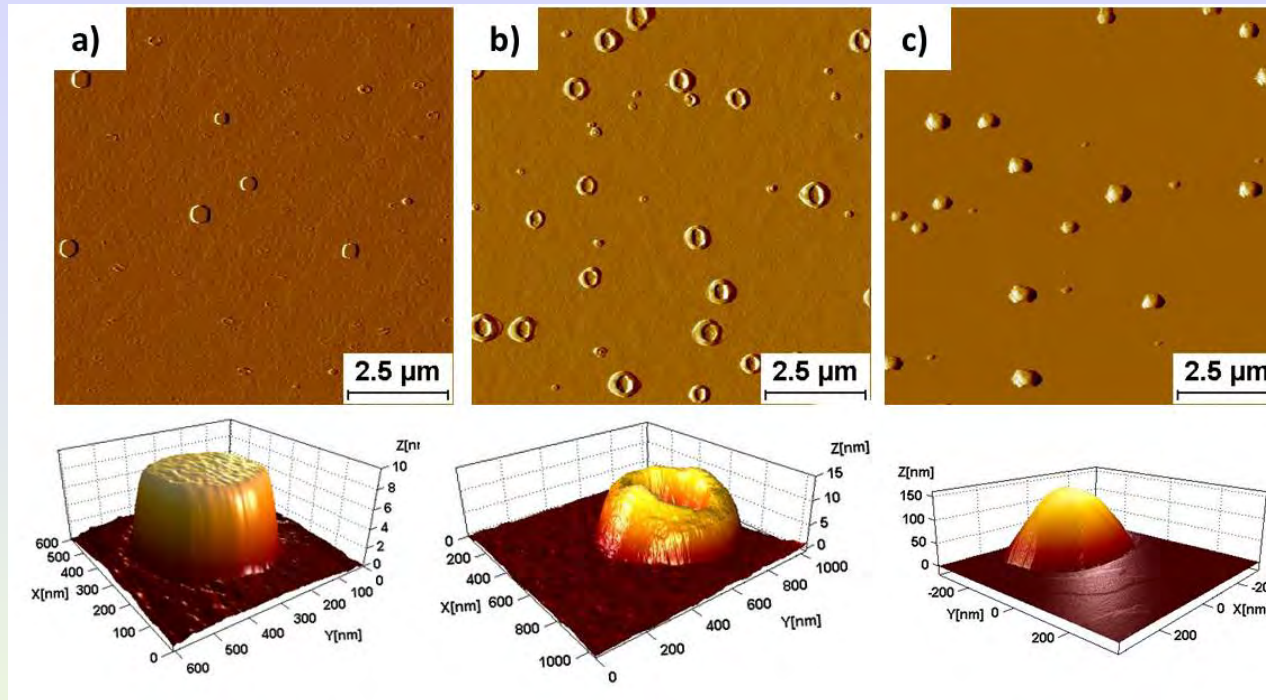
Back to surfaces...

$\text{Al}_{48\%}\text{In}_{52\%}\text{As}$ (2 nm) on InP

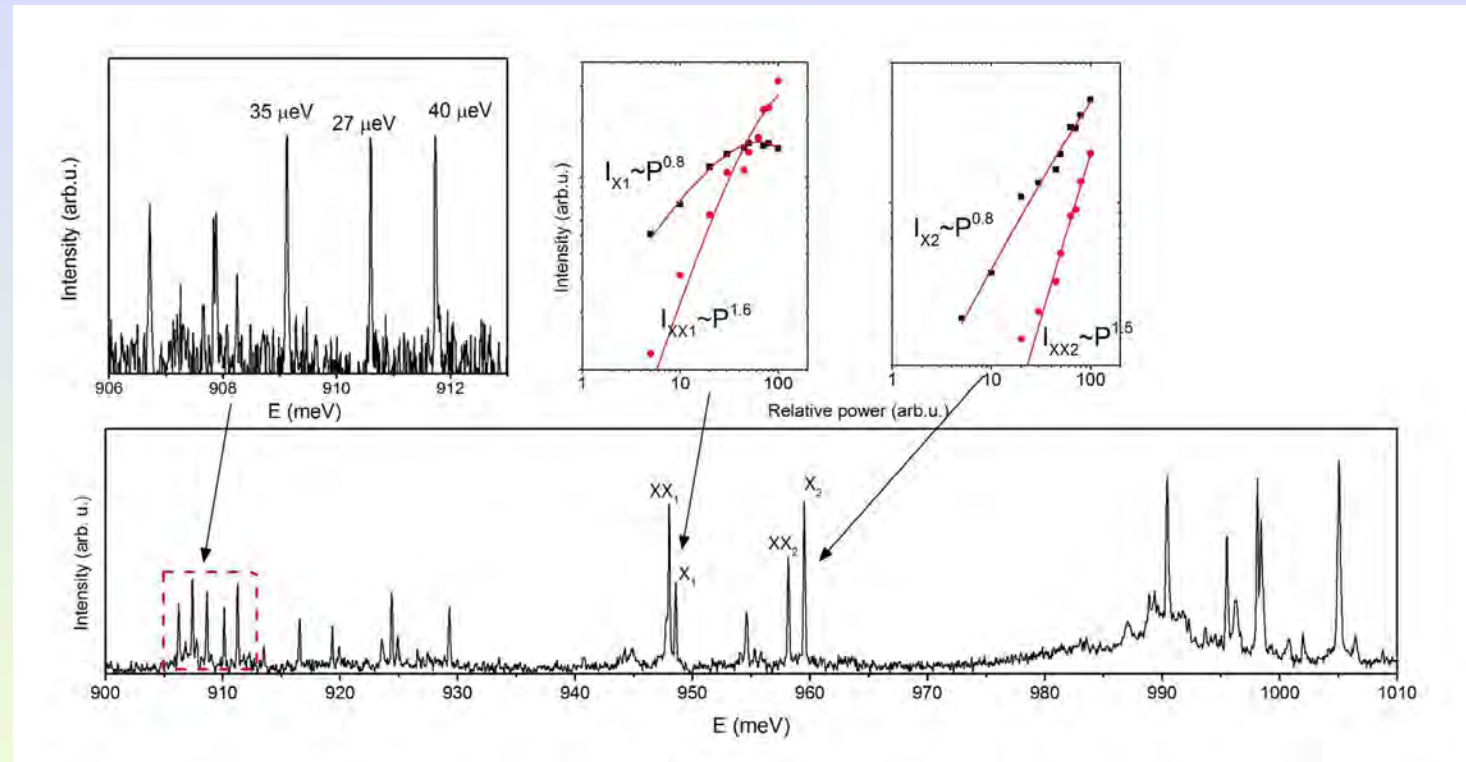




InP on Al_{48%}In_{52%}As

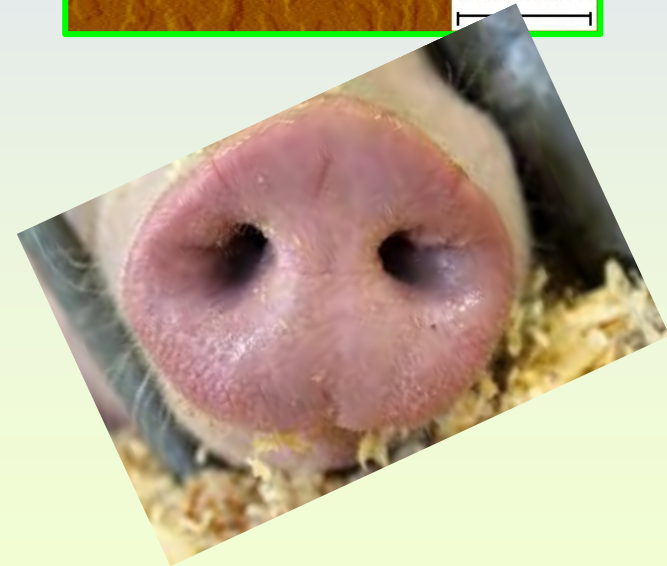
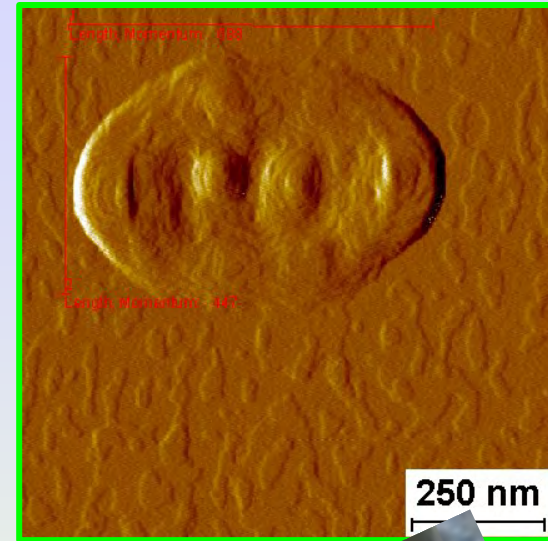
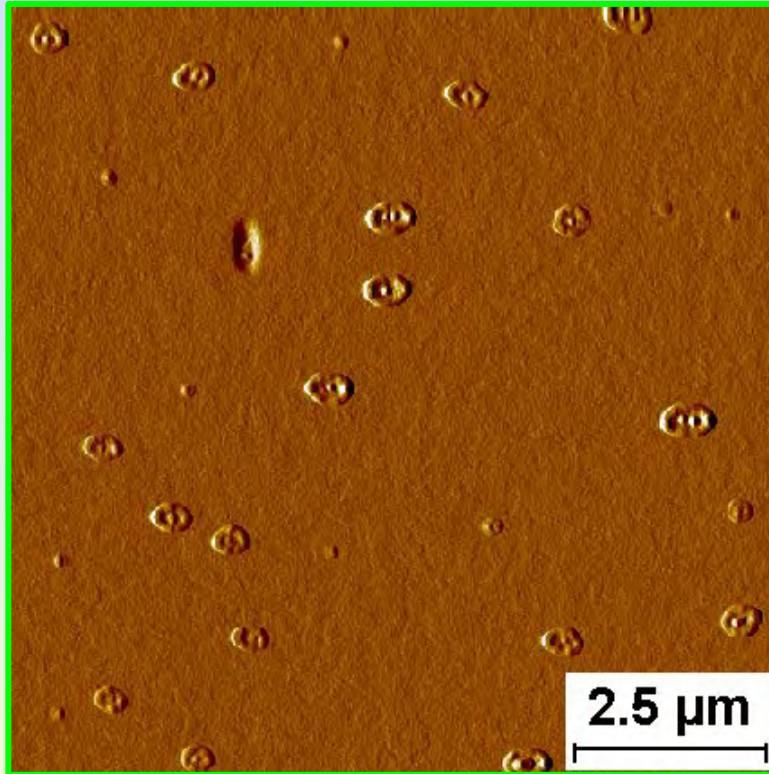


AFM morphologies (signal amplitudes) and corresponding zoom-in 3D reconstructions of 1nm InP layer deposited on LM AlInAs after 5sec mixed AsH₃ and PH₃ growth interruption. Samples grown on SO = (100) at T = 630 °C, Gr = 0.7 μ/h, V/III = 180 and then a) immediately cooled down under PH₃, b) exposed to AsH₃ at growth temperature for 5 minutes and then cooled down under PH₃, c) exposed to AsH₃ at growth temperature for 1 minute and then cooled down under AsH₃.



Part of the low temperature photoluminescence spectrum of nominally 1 nm InP in $\text{In}_{0.9}\text{Ga}_{0.1}\text{P}$ and $\text{Al}_{0.48}\text{In}_{0.52}\text{As}$ barriers, after exposing the QDs layer to arsine overflow. Top left insert shows zoom in to the spectrum detail with FWHM stated for each line, top central and right inserts show power dependence of the peak intensity, allowing for identification of the individual peaks as corresponding to exciton (X) and biexciton (XX) transitions.

And we....the quantum snout



Thanks

ER Epitaxy and Physics
of Nanostructures

IPIC
BRINGING PHOTONICS TO LIFE



sfi
science foundation Ireland
fondúireacht eolaíochta éireann

NDP
NATIONAL DEVELOPMENT PLAN

EUROPEAN REGIONAL DEVELOPMENT FUND



HEA
Higher Education Authority
An tUdarás um Ard-Oideachas



UCC
Coláiste na hOllscoile Corcaigh, Éire
University College Cork, Ireland